Lysophosphatidic Acid and IL-6 Trans-signaling Interact via YAP/TAZ and STAT3 Signaling Pathways in Human Trabecular Meshwork Cells

Felix Yemanyi and VijayKrishna Raghunathan

College of Optometry, University of Houston, Houston, Texas, United States

Correspondence: Felix Yemanyi, College of Optometry, University of Houston, 4901 Calhoun Road, 505 JDA Bldg, Rm 2195, Houston, TX 77204, USA; fyemanyi@central.uh.edu.
VijayKrishna Raghunathan, College of Optometry, University of Houston, 4901 Calhoun Road, Houston, TX 77204, USA; vraghunathan@uh.edu.

Received: September 12, 2020
Accepted: November 2, 2020
Published: November 20, 2020

Citation: Yemanyi F, Raghunathan V. Lysophosphatidic acid and IL-6 trans-signaling interact via YAP/TAZ and STAT3 signaling pathways in human trabecular meshwork cells. *Invest Ophthalmol Vis Sci.* 2020;61(13):29. https://doi.org/10.1167/iovs.61.13.29

Purpose. Lysophosphatidic acid (LPA) and soluble interleukin-6 receptor (sIL6R) are elevated in primary open angle glaucoma (POAG). LPA and IL6 modulate in response to biomechanical stimuli and converge on similar fibrotic phenotypes. Thus, we determined whether LPA and IL6 trans-signaling (IL6/sIL6R) interact via Yes-associated protein (YAP)/Transcriptional coactivator with a PDZ-binding motif (TAZ) or Signal transducer and activator of transcription 3 (STAT3) pathways in human trabecular meshwork (hTM) cells.

Methods. Confluent primary hTM cells were serum starved for 24 hours, and treated with vehicle, LPA (20 µM), IL6 (100 ng/mL)/sIL6R (200 ng/mL), or both (LPA + IL6/sIL6R) for 24 hours, with or without a YAP inhibitor (verteporfin; 2 µM) or STAT3 inhibitor (2 µM). Expression of key receptors and ligands, signaling mediators, actomyosin machinery, cell contractility, and extracellular matrix (ECM) targets of both signaling pathways was determined by immunocytochemistry, RT-qPCR, and Western blotting.

Results. LPA and IL6 trans-signaling coupling overexpressed/activated receptors and ligands, glycoprotein-130, IL6, and autotaxin; signaling mediators, YAP, TAZ, Pan-TEAD, and phosphorylated STAT3 (pSTAT3); actomyosin and contractile machinery components, myosin light chain 2 (MLC2), phosphorylated MLC2, rho-associated protein kinase 1, filamentous actin, and α-smooth muscle actin; and fibrotic ECM proteins, collagen I and IV, fibronectin, laminin, cysteine-rich angiogenic inducer 61, and connective tissue growth factor in hTM cells; mostly beyond LPA or IL6 trans-signaling alone. Verteporfin inhibited YAP, TAZ, and pSTAT3, with concomitant abrogation of aforementioned fibrotic targets; the STAT3 inhibitor was only partially effective.

Conclusions. These data suggest synergistic crosstalk between LPA and IL6 trans-signaling, mediated by YAP, TAZ, and pSTAT3. By completely inhibiting these mediators, verteporfin may be more efficacious in ameliorating LPA and/or IL6 trans-signaling–induced ocular hypertensive phenotypes in hTM cells.

Keywords: lysophosphatidic acid, IL-6 trans-signaling, YAP/TAZ pathway, STAT3 pathway, trabecular meshwork

Primary open angle glaucoma (POAG) is a leading cause of irreversible vision loss worldwide.[1–3] As the average life span continues to increase, glaucoma is expected to affect approximately 111.8 million people by 2040.[4] Elevated intraocular pressure (IOP) is the only major causative risk factor for POAG that is successfully targeted to delay either disease onset or progression.[5] An elevated IOP results from increased restriction to aqueous outflow, mainly owing to pathologic processes occurring at the trabecular meshwork (TM).[6–9] However, only a few IOP-lowering therapeutics directly target the TM.[10,11] The TM's pathobiology in POAG is broadly associated with increased extracellular matrix (ECM) accumulation,[12–17] increased actin contractility,[18] increased cross-linked actin networks,[19] and increased stiffness.[20,21] Although multiple factors may contribute to these TM pathologies, mounting evidence implicates aberrant levels of bioactive lipids, cytokines, or factors in the extracellular milieu and their associated dysregulated cell signaling pathways.[17,22–34]

For instance, the bioactive lipid, lysophosphatidic acid (LPA), is elevated in the aqueous humor of patients with POAG and other forms of glaucoma.[30,31,35,36] Apart from glaucoma, LPA has been implicated in cancer, fibrosis, and chronic inflammation[37–39]; and typically evokes its biological functions by binding to its G-protein–coupled receptors (i.e., LPAR1 to LPAR6).[33,38] LPA is a catalytic product of autotaxin (ATX), whose enzymatic activity and/or expression levels are also increased in POAG and mechanically stretched human TM (hTM) cells.[30] Small molecule inhibition of ATX leads to marked decrease of IOP in rabbits in vivo.[30] Moreover, perfusion of LPA or ATX in porcine or mice anterior segment organ cultures ex vivo decreases aqueous outflow facility, whereas inhibition of ATX increases aqueous outflow.[29,40] The desired outcome of LPA's or ATX's inhibition on

outflow facility is associated with decreases in actin stress fibers, focal adhesions, and myosin light chain phosphorylation.[30,31,33] More recently, the well-established mechanotransducers, Yes-associated protein (YAP) and Transcriptional coactivator with a PDZ-binding motif (TAZ),[41–44] have been identified as key downstream mediators of LPA-induced increased cell contractility and ECM deposition.[33] However, whether the LPA/YAP/TAZ signaling axis interacts with other mechanosensors to precipitate fibrotic phenotypes in hTM cells is not completely understood. Further, there is a paucity of knowledge in understanding whether LPA activates other signaling mediators or pathways apart from YAP/TAZ in hTM cells.

Like LPA, interleukin-6 (IL6) signaling has been implicated in cancer, fibrosis, and chronic inflammation[45–47] and may be involved in IOP regulation and glaucoma.[32,34,48,49] There are two main forms of IL6 signaling: classic and trans-signaling.[50] In classic signaling, IL6 binds to its membrane bound receptor (mIL6R), to form an IL6–mIL6R complex. This complex subsequently binds to the receptor subunit glycoprotein 130 (gp130) to activate the canonical Janus Kinase (JAK)/Signal Transducer and Activator of Transcription (STAT) or noncanonical pathways like mitogen-activated protein kinase (MAPK), which are important for desirable tissue regeneration and antibacterial benefits.[50,51] This finding suggests that classic signaling (if existent in the TM) may underpin the positive effect of IL6 on outflow facility in perfused porcine anterior segment organ cultures *ex vivo*,[34] given the loss of TM cellularity in elevated IOP.[52] However, in trans-signaling, typical of cells that do not constitutively express mIL6R, IL6 binds to the soluble form of mIL6R (i.e., sIL6R), which subsequently forms a complex with gp130 implicated in deleterious inflammatory malignancies.[50,51] Because sIL6R levels are elevated in the aqueous humor of patients with POAG resulting in an aberrant IL6 to sIL6R ratio compared with age-matched controls,[32] IL6 trans-signaling may be involved intricately in aqueous homeostasis.[34] However, the underlying mechanisms by which IL6 trans-signaling may influence ocular hypertensive phenotypes in hTM cells are not completely known.

Because LPA and IL6 modulate in response to biomechanical stimuli,[30,33,34] and their aberrant signaling converge on similar fibrotic outcomes,[37–39,45–47] there could be interaction between their respective signaling pathways. Such molecular and/or pathway crosstalk has previously been reported in cancerous nonocular cells.[53,54] Therefore, we hypothesized that there is crosstalk between LPA and IL6 trans-signaling via YAP/TAZ or STAT3 signaling pathways in precipitating fibrotic phenotypes in hTM cells. To test this hypothesis, we first documented the effect of LPA, IL6/sIL6R (trans-signaling), or both (LPA + IL6/sIL6R) on the expression of key receptors and ligands, signaling mediators, actomyosin machinery, cell contractility, and ECM targets of both signaling pathways. Subsequently, we determined the causal role of YAP/TAZ (using verteporfin, a YAP inhibitor) or STAT3 (using a STAT3 inhibitor) in LPA- and/or IL6 trans-signaling–mediated ocular hypertensive phenotypes in hTM cells.

Methods

Primary hTM Cell Isolation and Culture

Primary hTM cells were isolated from donor corneoscleral rims (age of donors ranged from 57 to 75 years of age) unsuitable for transplant (SavingSight Eye Bank, St. Louis, MO, USA), as described previously.[55] Donors had no known history of ocular diseases. This study is not considered a human subjects research because cells were acquired post-mortem from de-identified donor tissues. Therefore, it is deemed exempt by University of Houston's Institutional Review Board. However, all experiments were conducted in accordance with the tenets of the Declaration of Helsinki. Briefly, TM rings were cut into small pieces after successfully dissecting them from corneoscleral rims. These cut pieces were placed with 0.2% (w/v) collagen coated cytodex beads in complete growth medium (Dulbecco's modified Eagle medium/Nutrient Mixture F-12 [50:50] with 2.5 mM L-glutamine supplemented with 10% fetal bovine serum and 1% penicillin/amphotericin [Life Technologies, Carlsbad, CA, USA]). Cells that subsequently moved out of the TM were cultured in complete growth media and generally utilized between passages two and six. For characterization of primary hTM cells, all cell strains were subjected to dexamethasone-induced expression of myocilin as recommended.[55,56]

Subsequent Culture and Treatment of Primary hTM Cells

Primary hTM cells were cultured on plastic dishes or glass coverslips to confluency (approximately 90%) in 10% fetal bovine serum growth media. Cells were subsequently serum starved for 24 hours, after which respective treatment with vehicle control (veh), LPA (20 µM; catalog number: 10010093; Cayman Chemical, Ann Arbor, MI, USA), IL6 (100 ng/mL; catalog number: SRP3096; Sigma Aldrich, St. Louis, MO, USA)/sIL6R (200 ng/mL; catalog number: SRP3097; Sigma Aldrich, St. Louis, MO, USA), or both (LPA + IL6/sIL6R) in serum-free media was done for 24 hours. In another set of experiments, the aforementioned treatments were performed in the presence or absence of 2 µM verteporfin (YAP inhibitor, without light stimulation using aluminum foil; catalog number: 17334; Cayman Chemical, Ann Arbor, MI, USA) or 2 µM STAT3 inhibitor (Catalog number: 573097; Sigma Aldrich, St. Louis, MO, USA) in serum-free media for 24 hours. The concentration of verteporfin used in this study has previously been verified to be safe and efficacious in hTM cells and other ocular/nonocular cells.[57–59] Herein, we determined a safe and effective dose for the STAT3 inhibitor (that is, 2 µM) by performing a 3-(4,5-Dimethylthiazol-2-yl)-2,5-diphenyltetrazolium bromide assay (Supplementary Fig. S1) and Western blotting.

Quantitative Real-Time PCR

Total RNA was isolated from confluent hTM cells that had been treated with veh, LPA, IL6/sIL6R or both in serum-free media for 24 hours using an RNA purification kit (Catalog number: 12183025; PureLink RNA Mini kit, Invitrogen, Carlsbad, CA, USA). First-strand complementary DNA (cDNA) was synthesized using 1 µg of total RNA and the High-Capacity cDNA Reverse Transcription Kit (Catalog number: 4368813; Applied Biosystems, Foster City, CA, USA) with strict adherence to the manufacturer's instructions. Quantitative real-time PCR (qPCR) was performed on 20 ng of the cDNA with specific primers for receptors and ligands, signaling molecules, and intracellular and extracellular target genes

Investigative Ophthalmology & Visual Science

of LPA/YAP/TAZ and IL6 trans-signaling pathways (Supplementary Table S1) and the PowerUp SYBR Green Master Mix kit (Catalog number: A25918; Applied Biosystems, Foster City, CA, USA) in total volumes of 10 µL per reaction using a CFX Connect Real-time System from Bio-Rad Laboratories (Bio-Rad, Hercules, CA, USA). The cycle threshold (C_t) values were obtained from the qPCR equipment and analyzed using the $2^{-\Delta\Delta Ct}$ method, with glyceraldehyde 3-phosphate dehydrogenase (GAPDH) as an internal control gene.

Immunocytochemistry Analysis

After treatment of hTM cells cultured on glass coverslips with veh, LPA, IL6/sIL6 or both in serum-free media for 6 or 24 hours, respective samples were washed and fixed in 4% paraformaldehyde in phosphate buffered solution (PBS) at 4°C for 30 minutes, washed three times, 5 minutes each with PBS; permeabilized with 0.25% Triton X-100 in PBS (pH 7.4) for 10 minutes, and washed three times, each for 5 minutes. Then, blocking was done in 5% bovine serum albumin (BSA) in PBS for 30 minutes. Afterward, samples were incubated overnight at 4°C with primary antibodies; YAP, TAZ, and phosphorylated myosin light chain kinase (pMLC2) (Supplementary Table S2) respectively at 1/150 dilution in 5% BSA/PBS. After three 5-minute washes in PBS the following day, incubation was done with species-appropriate fluorophore-tagged secondary antibodies (Alexa Fluor 488 Anti-Rabbit and Anti-Mouse; Thermo Fisher Scientific, Waltham, MA, USA) and/or CF594-conjugated Phalloidin (catalog number: 00045; Biotium, Fremont, CA, USA), respectively, at a 1/500 dilution at room temperature for 1 hour. After three 5-minute washes, glass coverslips were mounted with Fluoromount-G Mounting Medium (Catalog number: 0100-01; Southern Biotech, Birmingham, AL, USA) onto slides. Subsequently, immunofluorescent images were captured with Zeiss LSM 800 laser scanning confocal microscope (Carl Zeiss, Jena, Germany) with a 20× objective. For each immunolabelled glass coverslip, 5 to 10 random locations were imaged. At least three glass coverslips were used for each immunolabeling condition for each cell strain with the same imaging settings for cohorts.

Western Blot Analysis

Serum-starved confluent hTM cells treated with veh, LPA, IL6/sIL6R, or both with or without a YAP or STAT3 inhibitor for 24 hours were lysed and scraped into radioimmunoprecipitation assay buffer (ThermoScientific, Waltham, MA, USA) supplemented with protease and phosphatase inhibitors (Fisher Scientific, Hampton, NH, USA) on ice, and subsequently centrifuged at 12,000*g* for 15 minutes at 4°C to pellet and remove any cellular debris. Supernatants were transferred into fresh tubes and quantified via a modified Lowry assay (DC assay; Biorad, Hercules, CA, USA) with BSA as the standard. Then, protein lysates were denatured in a 1:10 mixture of 2-mercaptoethanol and 4× Laemmli buffer by boiling at 100°C for 5 minutes. After quickly centrifuging proteins at 15,000*g* for 30 seconds, equal amounts of protein were loaded per well (20 µg) for each sample and ran on denaturing 4% to 15% gradient polyacrylamide ready-made gels (Biorad); subsequently transferred onto polyvinylidene difluoride membranes by electrophoresis. Membrane blots were blocked in 5% BSA in 1× Tris-buffered saline/tween-20 (TBST) for 1 hour. Immunoblots were incubated overnight at 4°C with specific primary antibodies (Supplementary Table S2) on a rotating shaker. The membrane blot was washed thrice with TBST; each wash lasting for approximately 10 minutes. Subsequent incubation with corresponding horseradish peroxidase–conjugated species-specific secondary antibodies (Supplementary Table S2) for 45 minutes was done, followed by three 10-minute washes with TBST. The protein bands were then detected using enhanced chemiluminescence detection reagents (SuperSignal West Femto Maximum Sensitivity Substrate; Life Technologies, Grand Island, NY, USA) and imaged with a Bio-Rad ChemiDoc MP imaging system. Respective membrane blots were stripped and probed with GAPDH as a housekeeping protein. Data were exported into ImageJ for densitometric analysis.

Data Analysis

A one-way ANOVA followed by Tukey multiple comparisons post hoc test was used for analyzing gene and protein expression data among experimental groups, with P values of less than 0.05 deemed to be statistically significant. All data are presented as mean ± standard error of the mean (SEM), in bar graphs, representative immunofluorescent micrographs, and blots where applicable.

Results

LPA and/or IL6 Trans-Signaling Differentially Overexpressed Their Specific Receptors and Ligands in hTM Cells

The biological functions of both LPA and IL6 trans-signaling in physiology or disease are typically initiated via overexpression/activation of their specific receptors and/or ligands.[38,50] Thus, we first determined the effect of LPA, or IL6 trans-signaling, or their interaction on the gene expression of pathway receptors (e.g., *LPAR1* to *LPAR6*, *IL6 receptor* [*IL6R*], and *gp130*), and ligands (e.g., ATX and IL6) in hTM cells after 24 hours via qPCR. Compared with veh, only LPA-treated hTM cells showed a small yet statistically significant increase of *LPAR1* ($P < 0.01$; Fig. 1A). In addition, whereas LPA alone markedly decreased *LPAR2* ($P < 0.001$) in hTM cells, IL6/sIL6R alone slightly increased its expression ($P < 0.05$; Fig. 1B) beyond LPA alone or LPA + IL6/sIL6R. Further, IL6/sIL6R alone significantly decreased *LPAR3* ($P < 0.001$), whereas LPA alone or LPA + IL6/sIL6R had no effect on its expression (Fig. 1C). Only LPA-treated hTM cells showed an increased expression of *LPAR4* ($P < 0.01$), whereas the other experimental groups were not any different from veh (Fig. 1D). Whereas LPA alone and LPA + IL6/sIL6R slightly decreased *LPAR6*, IL6/sIL6R alone significantly increased its expression beyond LPA alone or LPA + IL6/sIL6R (Fig. 1E). Moreover, compared with veh, there were no differences in *IL6R* levels among groups (Fig. 1F), whereas *gp130* was markedly increased by IL6/sIL6R alone or LPA + IL6/sIL6R ($P < 0.001$, respectively), markedly beyond LPA alone, which showed no difference (Fig. 1G). Associated with these changes in receptors was an increased expression of *ATX* by LPA + IL6/sIL6R ($P < 0.001$), significantly beyond LPA alone or IL6/sIL6R alone, which were not any different from veh (Fig. 1H). Finally, IL6/sIL6R alone or LPA + IL6/sIL6R significantly upregulated *IL6* in hTM cells ($P < 0.001$, respectively), profoundly beyond LPA alone, which increased IL6, but did not reach significance (Fig. 1I).

Investigative Ophthalmology & Visual Science

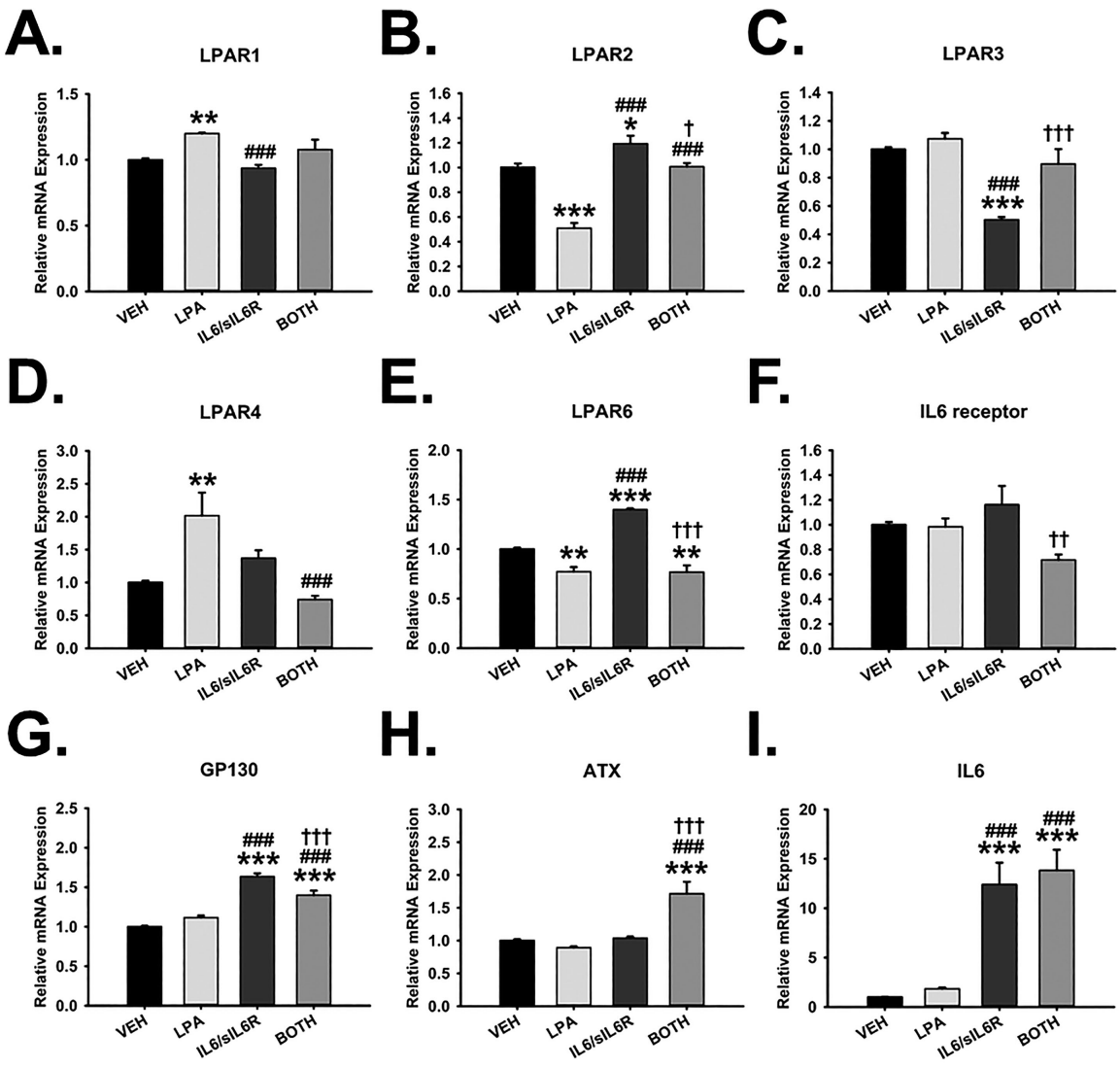

Figure 1. LPA and/or IL6 trans-signaling differentially modulate key pathway receptors and ligands. Confluent primary hTM cells were serum starved for 24 hours and then treated with veh, LPA (20 μM), IL6 (100 ng/mL)/sIL6R (200 ng/mL), or both (LPA + IL6/sIL6R) for 24 hours. RNA was subsequently extracted for reverse transcription and qPCR. GAPDH was used as an internal control for normalization. Respective bar graph for the gene expression of (**A**) LPAR1, (**B**) LPAR2, (**C**) LPAR3, (**D**) LPAR4, (**E**) LPAR6, (**F**) IL6 receptor, (**G**) GP130, (**H**) ATX, and (**I**) IL6. Columns and error bars are the means and standard error of mean (SEM). One-way ANOVA with the Tukey pairwise comparisons post hoc test was used for statistical analysis. ($n = 3$ biological replicates; $^{*}P < 0.05$, $^{**}P < 0.01$, $^{***}P < 0.001$ for the group of interest versus veh; $^{\#\#\#}P < 0.001$ for the group of interest versus LPA; $^{\dagger}P < 0.05$, $^{\dagger\dagger}P < 0.01$, $^{\dagger\dagger\dagger}P < 0.001$ for the group of interest versus IL6/sIL6R). LPA, Lysophosphatidic acid; hTM, Human trabecular meshwork; veh, Vehicle control; IL6, Interleukin-6; sIL6R, Soluble IL6 receptor; GAPDH, Glyceraldehyde 3-phosphate dehydrogenase; LPAR, LPA receptor; GP130, Glycoprotein 130; ATX, Autotaxin.

LPA and/or IL6 Trans-Signaling Increased Expression of YAP/TAZ and STAT3 Signaling Mediators in hTM Cells

Because the interaction between LPA and IL6/sIL6R resulted in an overexpression of the *gp130*, *ATX*, and *IL6* genes, our initial confidence in a probable crosstalk between their respective signaling pathways soared. Thus, because both LPA and IL6 modulate in response to mechanical stimuli,[30,33,34] and the mechanotransducers, YAP and TAZ, have been implicated in LPA-induced diseased phenotypes,[33] we determined the effect of LPA and/or IL6/sIL6R on signaling mediators of the YAP/TAZ pathway in hTM cells by immunocytochemistry, qPCR, and Western blotting analyses.

We discovered that, compared with veh, YAP and TAZ were localized in the nucleus of hTM cells treated with LPA, or IL6/sIL6R, or their interaction (Fig. 2A and 2B, respectively).

Further, compared with veh, LPA, or IL6/sIL6R, or LPA + IL6/sIL6 significantly elevated YAP ($P < 0.01$, $P < 0.05$, and $P < 0.001$, respectively) and phosphorylated YAP (pYAP) ($P < 0.001$, respectively) in hTM cells (Fig. 2C and 2D, respectively). Additionally, TAZ was markedly increased by IL6/sIL6R alone or its interaction with LPA ($P < 0.05$, respectively), whereas LPA alone upregulated TAZ's expression without attaining significance (Fig. 2E). Phosphorylated TAZ (pTAZ) was also significantly overexpressed by LPA, or IL6/sIL6R, or their interaction ($P < 0.05$, $P < 0.001$, and $P < 0.001$, respectively) in hTM

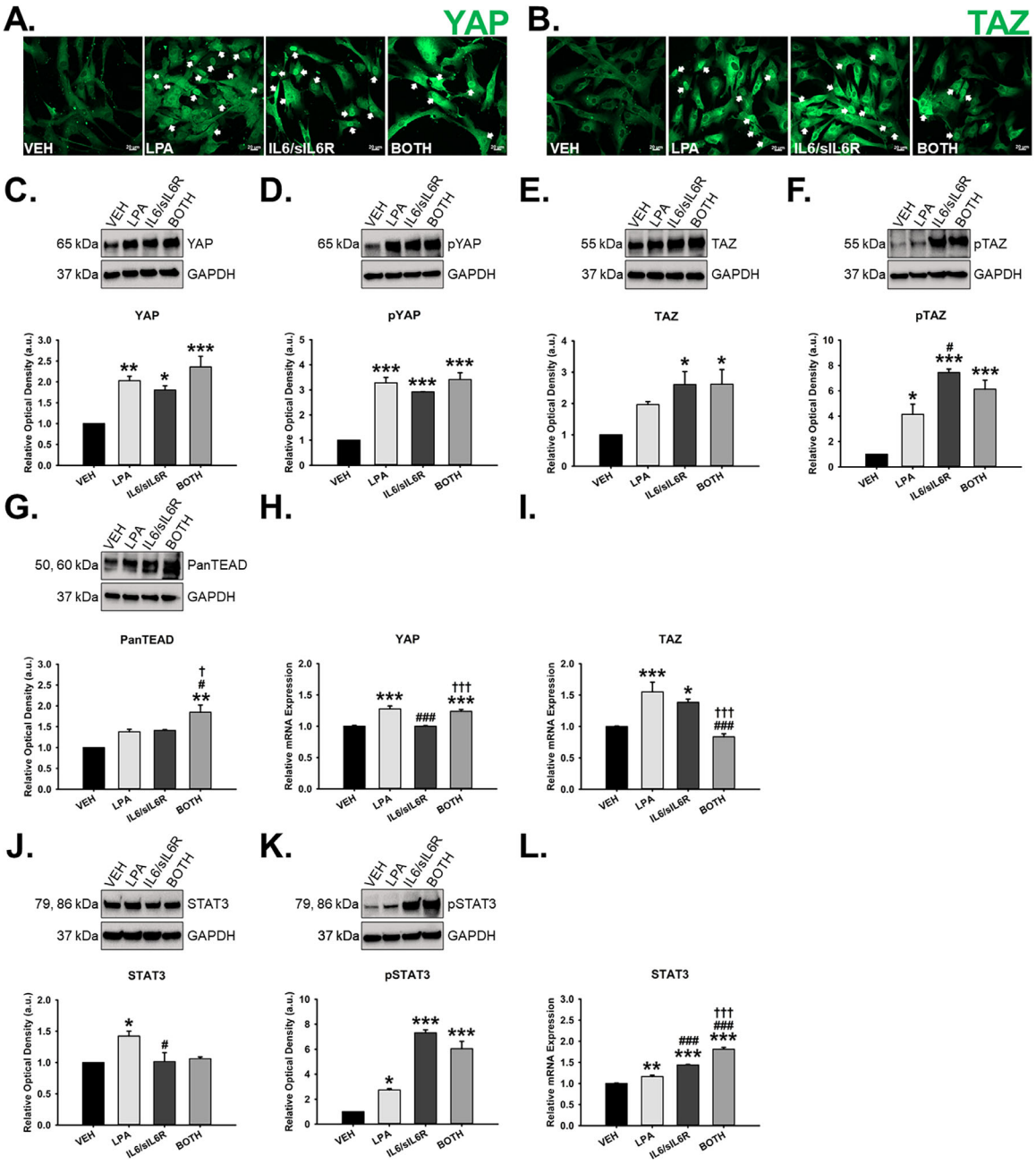

Figure 2. LPA and/or IL6 trans-signaling overexpressed signaling mediators of YAP/TAZ and STAT3 pathways in hTM cells. Confluent primary hTM cells were serum starved for 24 hours and then treated with veh, LPA (20 µM), IL6 (100 ng/mL)/sIL6R (200 ng/mL), or both (LPA + IL6/sIL6R) for 6 or 24 hours. Immunocytochemistry was performed, and RNA and protein were extracted for qPCR and Western blot analyses, respectively. GAPDH was used as a housekeeping gene/protein for normalization. Representative micrographs showing (**A**) YAP's immunolabeling and (**B**) TAZ's immunolabeling. Representative blot (*top*) and densitometric analysis (*bottom*) or bar graphs of (**C**) YAP protein, (**D**) pYAP, (**E**) TAZ protein, (**F**) pTAZ, (**G**) Pan-TEAD, (**H**) YAP gene, (**I**) TAZ gene, (**J**) STAT3 protein, (**K**) pSTAT3, and (**L**) STAT3 gene. Columns and error bars are means and standard error of mean (SEM). One-way ANOVA with the Tukey pairwise comparisons post hoc test was used for statistical analysis. ($n = 3$ biological replicates; $^{*}P < 0.05$, $^{**}P < 0.01$, $^{***}P < 0.001$ for the group of interest versus veh; $^{\#}P < 0.05$, $^{\#\#\#}P < 0.001$ for the group of interest versus LPA; $^{\dagger}P < 0.05$, $^{\dagger\dagger\dagger}P < 0.001$ for the group of interest versus IL6/sIL6R). LPA, Lysophosphatidic acid; hTM, Human trabecular meshwork; veh, Vehicle control; IL6, Interleukin-6; sIL6R, Soluble IL6 receptor; GAPDH, Glyceraldehyde 3-phosphate dehydrogenase; YAP, Yes-associated protein; pYAP, Phosphorylated YAP; TAZ, Transcriptional co-activator with a PDZ-binding motif; pTAZ, Phosphorylated TAZ; Pan-TEAD, Pan-transcriptional enhancer factor domain; STAT3, Signal transducer and activator of transcription 3; pSTAT3 Phosphorylated STAT3. Scale bar, 20 µm.

cells (Fig. 2F). Moreover, only LPA + IL6/sIL6R markedly upregulated the Pan-transcriptional enhancer factor-domain (Pan-TEAD; $P < 0.01$) in hTM cells, beyond LPA alone or IL6/sIL6 alone, which showed no difference (Fig. 2G). However, at the mRNA level, *YAP* was significantly increased by LPA alone or its interaction with IL6/sIL6R ($P < 0.001$, respectively), whereas *TAZ* was markedly upregulated by LPA alone or IL6/sIL6R alone ($P < 0.001$ and

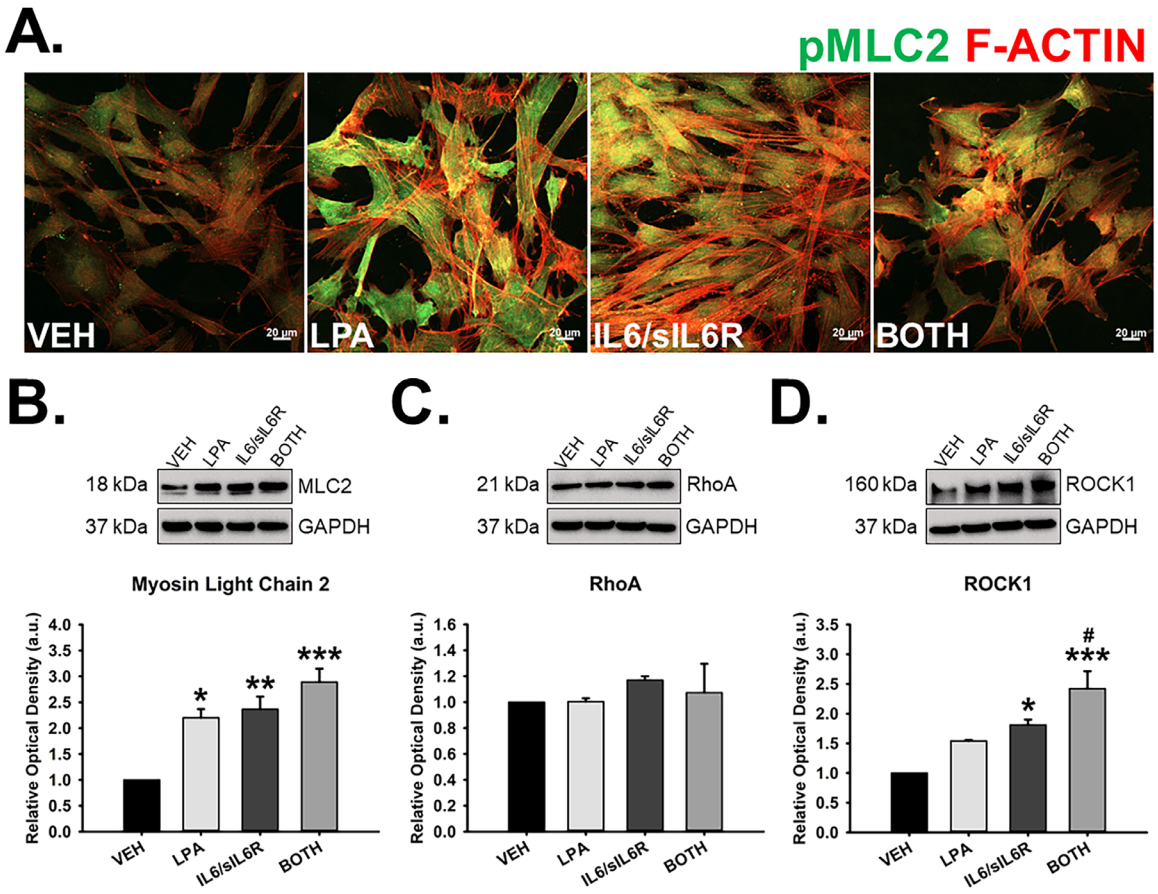

Figure 3. LPA and/or IL6 trans-signaling overexpressed key components of the actomyosin machinery in hTM cells. Primary hTM cells were cultured to confluency in complete medium, serum starved for 24 hours, and then treated with veh, LPA (20 μM), IL6 (100 ng/mL)/sIL6R (200 ng/mL), or both (LPA + IL6/sIL6R) for 24 hours. Immunocytochemistry was performed and protein was extracted for Western blot analysis. GAPDH was used as a housekeeping protein for normalization. Representative micrographs showing (**A**) Immunolabeling for pMLC2 and F-ACTIN. Representative blot (*top*) and densitometric analysis (*bottom*) of (**B**) MLC2, (**C**) RhoA, and (**D**) ROCK1. Columns and error bars are the means and standard error of mean (SEM). One-way ANOVA with the Tukey pairwise comparisons post hoc test was used for statistical analysis. ($n = 3$ biological replicates; $^{*}P < 0.05$, $^{**}P < 0.01$, $^{***}P < 0.001$ for the group of interest versus veh; $^{\#}P < 0.05$ for the group of interest versus LPA). LPA, Lysophosphatidic acid; hTM, Human trabecular meshwork; veh, Vehicle control; IL6, Interleukin-6; sIL6R, Soluble IL6 receptor; F-ACTIN, Filamentous actin; GAPDH, Glyceraldehyde 3-phosphate dehydrogenase. MLC2, Myosin light chain 2; pMLC2, Phosphorylated MLC2. RhoA, Ras homolog family member A; ROCK1, Rho-associated coiled-coil protein kinase 1. Scale bar, 20 μm.

$P < 0.05$, respectively), markedly beyond LPA + IL6/sIL6R, which was not any different from veh (Fig. 2H and 2I, respectively).

Further, STAT3 is established as a potent downstream mediator of the fibrotic effects of IL6 trans-signaling in cells.[51] Therefore, because LPA and IL6 trans-signaling converge on similar fibrotic phenotypes,[37,39,45,47] we next determined the effect of LPA, or IL6/slIL6R, or their combinatory effects on STAT3 molecules. Compared with veh, only LPA alone significantly overexpressed STAT3 ($P < 0.05$) in hTM cells, whereas the other experimental groups showed no difference (Fig. 2J). However, phosphorylated STAT3 (pSTAT3) was significantly upregulated by LPA alone, or IL6/sIL6R alone, or their interaction ($P < 0.05$, $P < 0.001$, and $P < 0.001$, respectively) in hTM cells (Fig. 2K). However, at the mRNA level, *STAT3* was significantly increased by LPA alone, or IL6/sIL6R alone, or their interaction; LPA + IL6/sIL6R was markedly increased beyond LPA alone or IL6/sIL6R alone (Fig. 2L).

LPA and/or IL6 Trans-Signaling Overexpressed Key Components of the Actomyosin Machinery in hTM Cells

Because contractile properties of the cell's actomyosin machinery contribute significantly to the biological events (e.g., fibrotic phenotypes) of YAP/TAZ- and/or STAT3-dependent signaling pathways,[33,41,60,61] next, we determined the effect of LPA, or IL6/sIL6R, or their interaction on key components of the actin cytoskeleton via immunocytochemistry and Western blotting analyses. As shown in Figure 3A via immunocytochemistry, compared with veh, there was increased expression/colocalization of phosphorylated myosin light chain kinase 2 (pMLC2) and filamentous actin (F-actin) in hTM cells treated with LPA, or IL6/sIL6R, or their interaction for 24 hours. Accompanying this, MLC2 protein was significantly overexpressed in hTM cells treated with LPA alone, IL6/sIL6R alone, or LPA + IL6/sIL6R ($P < 0.05$, $P < 0.01$, and $P < 0.001$, respectively) (Fig. 3B). Further,

Investigative Ophthalmology & Visual Science

none of the experimental groups significantly impacted the expression of Ras homolog family member A (RhoA) in hTM cells (Fig. 3C). However, IL6/sIL6R alone or its interaction with LPA significantly upregulated Rho-associated coiled-coil protein kinase 1 (ROCK1) ($P < 0.05$ and $P < 0.001$, respectively) in hTM cells, beyond LPA alone, which increased its expression, but without statistical significance (Fig. 3D).

LPA and/or IL6 Trans-Signaling Increased Cell Contractility and Key Target ECM Proteins/Genes of YAP/TAZ and STAT3 Pathways in hTM Cells

Given that LPA and/or IL6 trans-signaling triggered specific receptors and ligands, signaling mediators, and key components of the actomyosin machinery of YAP/TAZ- and/or STAT3-mediated pathways, next, we determined changes in their respective fibrotic targets (i.e., intracellular and extracellular) in hTM cells via Western blotting and qPCR analyses. We found that LPA, or IL6/sIL6R, or LPA + IL6/sIL6R markedly overexpressed α-smooth muscle actin (α-SMA) ($P < 0.001$, respectively) in hTM cells compared with veh; the increase by LPA or its interaction with IL6/sIL6R was significantly beyond that of IL6/sIL6R alone (Fig. 4A). In addition, LPA, or IL6/sIL6R, or their interaction significantly overexpressed collagen I ($P < 0.01$, $P < 0.001$, and $P < 0.05$, respectively) in hTM cells relative to veh; LPA alone or its interaction with IL6/sIL6R was markedly lesser than IL6/sIL6R alone (Fig. 4B). Further, whereas LPA alone had no effect on the expression of fibronectin, IL6/sIL6R alone or LPA + IL6/sIL6R markedly upregulated its expression ($P < 0.001$, respectively) in hTM cells (Fig. 4C). Moreover, whereas LPA alone or its interaction with IL6/sIL6R significantly increased laminin ($P < 0.01$ and $P < 0.05$, respectively) in hTM cells, the increase by IL6/sIL6R alone was not significant (Fig. 4D). Also, LPA, or IL6/sIL6R, or LPA + IL6/sIL6R markedly overexpressed cysteine-rich angiogenic inducer 61 (CYR61) ($P < 0.05$, $P < 0.01$, and $P < 0.001$, respectively) in hTM cells (Fig. 4E). Similarly, whereas LPA alone or IL6/sIL6R alone markedly upregulated connective tissue growth factor (CTGF) ($P < 0.001$ and $P < 0.01$, respectively) in hTM cells, LPA + IL6/sIL6R did not (Fig. 4F). However, at the mRNA level, whereas LPA or its interaction with IL6/sIL6R showed no difference in *α-SMA* expression, IL6/sIL6R alone significantly decreased its levels ($P < 0.001$) relative to veh (Fig. 4G). Further, *collagen I* and *collagen IV* mRNA were significantly increased in hTM cells by LPA alone ($P < 0.001$, respectively), whereas IL6/sIL6R alone markedly decreased its expression ($P < 0.001$, respectively), with no effect by LPA + IL6/sIL6R (Figs. 4H and 4I, respectively). Moreover, the expression of *fibronectin* mRNA was not any different among experimental groups compared with veh (Fig. 4J). Additionally, LPA, or IL6/sIL6R or their interaction significantly increased the gene expression of *CYR61* ($P < 0.001$, respectively) relative to veh, consistent with the observation at its protein level. The increase by LPA + IL6/sIL6R was markedly beyond that of IL6/sIL6R alone (Fig. 4K). Finally, only LPA alone markedly overexpressed *CTGF* mRNA in hTM cells, whereas IL6/sIL6R alone significantly decreased its expression, with no marked effect by LPA + IL6/sIL6R relative to veh (Fig. 4L).

Verteporfin Differentially Downregulated Key Signaling Mediators of YAP/TAZ and STAT3 Pathways Induced by LPA and/or IL6 Trans-Signaling in hTM Cells

Before establishing the causal role of YAP/TAZ in LPA-induced and/or IL6 trans-signaling–induced fibrotic phenotypes in hTM cells, next, we determined the effect of verteporfin[58,59] (a YAP inhibitor) on LPA- and/or IL6 trans-signaling–mediated expression of signaling mediators of YAP/TAZ and STAT3 pathways in hTM cells. We found that, in the absence of verteporfin, YAP was significantly increased by LPA alone, or IL6/sIL6R alone, or their interaction ($P < 0.001$, $P < 0.001$, and $P < 0.01$, respectively) in hTM cells compared with veh. However, in the presence of verteporfin, unsurprisingly, YAP was significantly downregulated by veh, or LPA, or LPA + IL6/sIL6R ($P < 0.001$, respectively), whereas IL6/sIL6R showed no marked difference (Fig. 5A). In addition, in the absence of verteporfin, relative to veh, whereas IL6/sIL6R alone or its interaction with LPA significantly increased pYAP ($P < 0.05$ and $P < 0.001$, respectively) in hTM cells, the increase by LPA alone was not significant. However, in the presence of verteporfin, all the experimental groups had no significant effect on the expression of pYAP relative to veh (Fig. 5B).

Further, in the absence of verteporfin, LPA, or IL6/sIL6R, or their interaction markedly overexpressed TAZ ($P < 0.001$, respectively) in hTM cells; LPA + IL6/sIL6R was further heightened beyond LPA alone. However, in the presence of verteporfin, TAZ was significantly decreased by all the experimental groups ($P < 0.001$, respectively) compared with veh (Fig. 5C). Moreover, in the absence of verteporfin, all the experimental groups markedly overexpressed pTAZ in hTM cells. In the presence of verteporfin, whereas veh or LPA + IL6/sIL6R had no significant effect on pTAZ, LPA alone or IL6/sIL6R alone significantly decreased its expression ($P < 0.01$ and $P < 0.001$, respectively) (Fig. 5D). Also, in the absence of verteporfin, all the experimental groups significantly upregulated Pan-TEAD ($P < 0.001$, respectively) in hTM cells; LPA + IL6/sIL6R was significantly increased beyond LPA alone. However, in the presence of verteporfin, there was no difference in the expression of Pan-TEAD among the groups relative to veh (Fig. 5E). Similarly, in the absence of verteporfin, STAT3 was significantly increased by all the experimental groups ($P < 0.05$, $P < 0.01$, and $P < 0.001$, respectively) compared with veh. However, in verteporfin's presence, none of the experimental groups markedly impacted STAT3's expression relative to veh (Fig. 5F). Finally, without verteporfin, IL6/sIL6R alone or its interaction with LPA significantly increased pSTAT3 ($P < 0.001$, respectively) in hTM cells; LPA-IL6/sILR6 interaction was markedly increased beyond LPA alone or IL6/sIL6R alone. However, with verteporfin, none of the groups showed significant effects on pSTAT3's expression (Fig. 5G).

Verteporfin Downregulated Key Components of the Actomyosin Machinery Induced by LPA and/or IL6 Trans-Signaling in hTM Cells

After confirming the inhibitory effects of verteporfin on signaling mediators of YAP/TAZ and STAT3 pathways, next, we determined the causal role of this inhibitor on LPA-mediated and/or IL6 trans-signaling–mediated protein

Investigative Ophthalmology & Visual Science

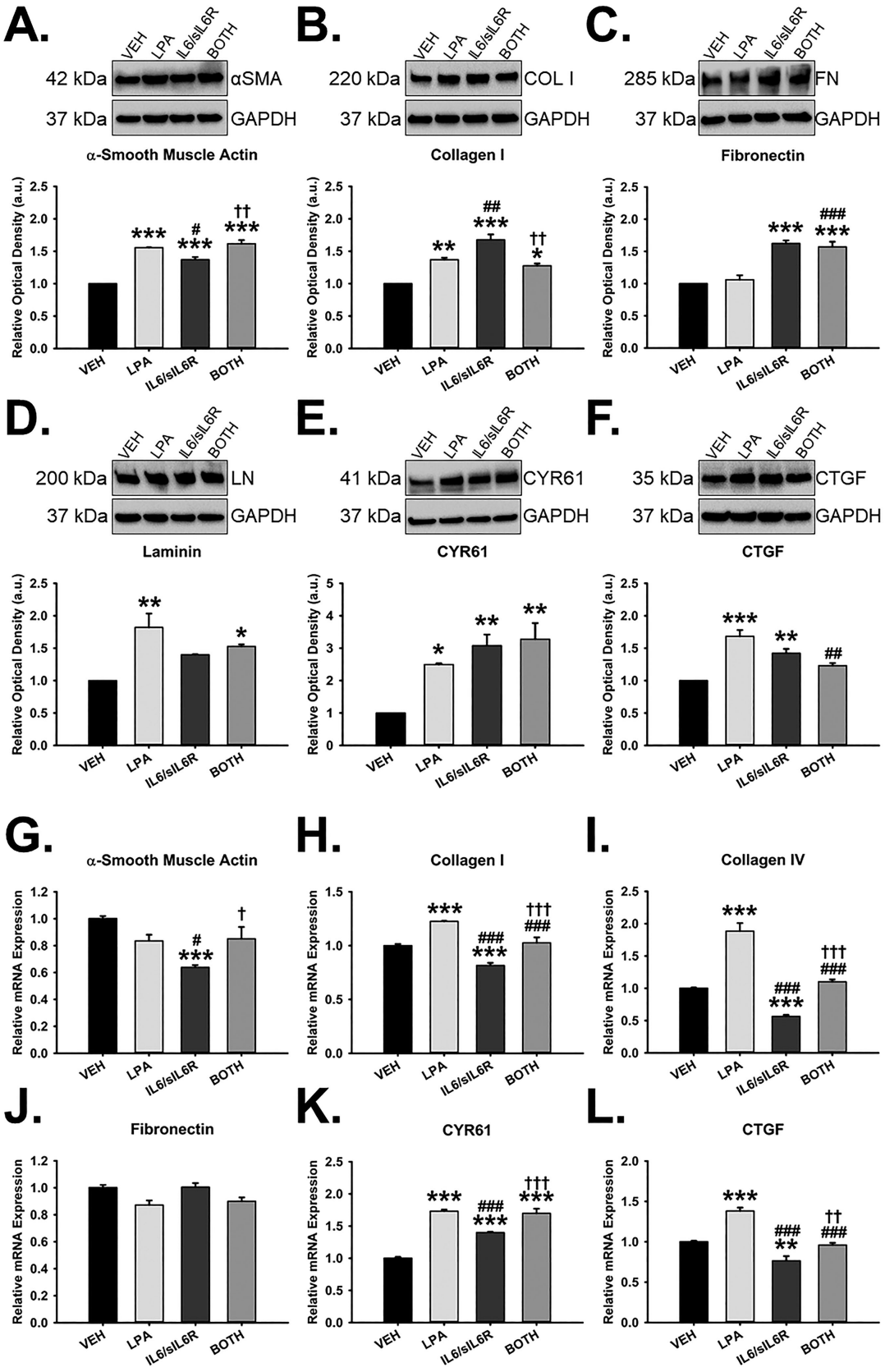

Figure 4. LPA and/or IL6 trans-signaling increased cell contractility and target ECM proteins in hTM cells. Confluent primary hTM cells were serum starved for 24 hours and then treated with veh, LPA (20 μM), IL6 (100 ng/mL)/sIL6R (200 ng/mL), or both (LPA + IL6/sIL6R) for 24 hours. RNA and protein were extracted for qPCR and Western blot analyses respectively. GAPDH was used as a housekeeping gene/protein for normalization. Representative blot (*top*) and densitometric analysis (*bottom*) of (**A**) α-Smooth Muscle Actin, (**B**) Collagen I (**C**) Fibronectin, (**D**) Laminin, (**E**) CYR61, and (**F**) CTGF. Representative bar graphs of (**G**) α-Smooth Muscle Actin gene (**H**) Collagen I gene,

(**I**) Collagen IV gene, (**J**) Fibronectin gene, (**K**) CYR61 gene, and (**L**) CTGF gene. Columns and error bars are the means and standard error of mean (SEM). One-way ANOVA with the Tukey pairwise comparisons post hoc test was used for statistical analysis. ($n = 3$ biological replicates; $^{*}P < 0.05$, $^{**}P < 0.01$, $^{***}P < 0.001$ for the group of interest versus veh; $^{\#}P < 0.05$, $^{\#\#}P < 0.01$, $^{\#\#\#}P < 0.001$ for the group of interest versus LPA; $^{\dagger}P < 0.05$, $^{\dagger\dagger}P < 0.01$, $^{\dagger\dagger\dagger}P < 0.001$ for the group of interest versus IL6/sIL6R). ECM, Extracellular matrix; LPA, Lysophosphatidic acid; hTM, Human trabecular meshwork; veh, Vehicle control; IL6, Interleukin-6; sIL6R, Soluble IL6 receptor; GAPDH, Glyceraldehyde 3-phosphate dehydrogenase; CYR61, Cysteine-rich angiogenic inducer 61; CTGF, Connective tissue growth factor.

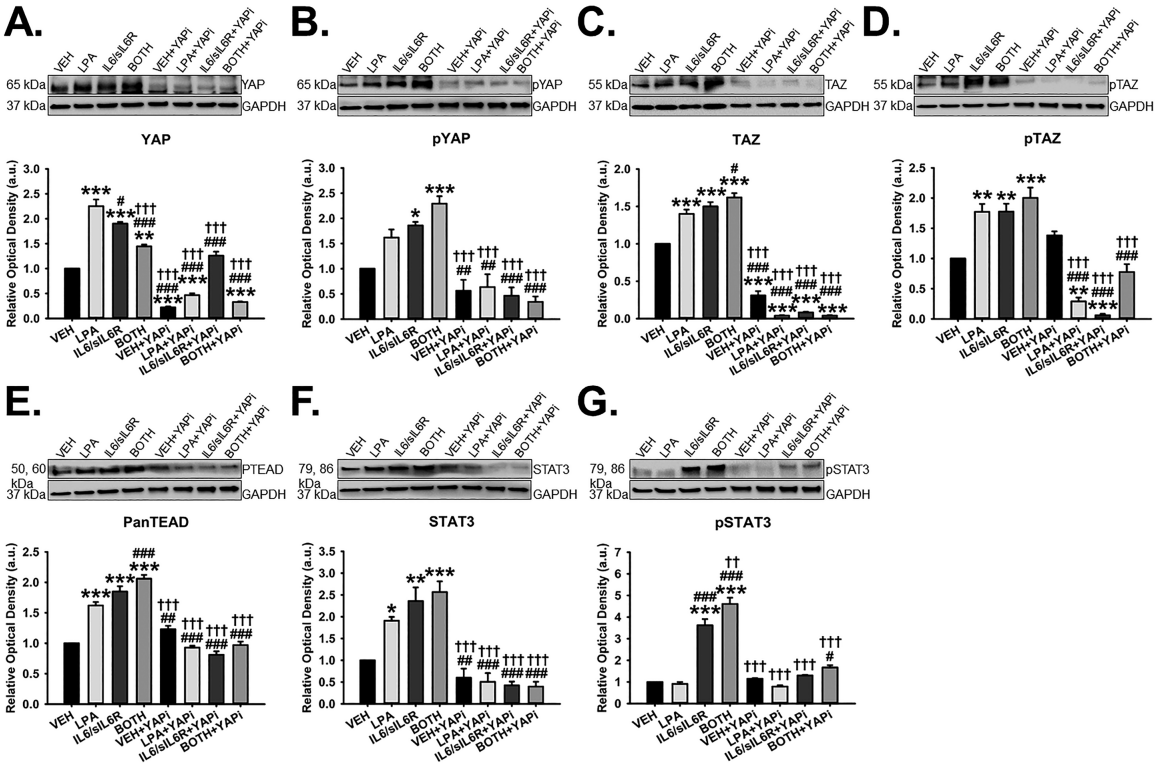

Figure 5. Verteporfin downregulated LPA- and/or IL6 trans-signaling–mediated overexpression of signaling mediators of YAP/TAZ and STAT3 in hTM cells. Primary hTM cells were cultured to confluency in complete medium, serum starved for 24 hours, and then treated with veh, LPA (20 µM), IL6 (100 ng/mL)/sIL6R (200 ng/mL), or both (LPA + IL6/sIL6R) in the presence or absence of 2 µM verteporfin (YAP inhibitor) for 24 hours. Protein was isolated for Western blot analysis. GAPDH was used as an internal control for protein normalization. Representative blot (*top*) and densitometric analysis (*bottom*) of (A) YAP, (B) pYAP, (C) TAZ, (D) pTAZ, (E) Pan-TEAD, (F) STAT3, and (G) pSTAT3. Columns and error bars are the means and standard error of mean (SEM). One-way ANOVA with the Tukey pairwise comparisons post hoc test was used for statistical analysis. ($n = 3$ biological replicates; $^{*}P < 0.05$, $^{**}P < 0.01$, $^{***}P < 0.001$ for the group of interest versus veh; $^{\#}P < 0.05$, $^{\#\#\#}P < 0.001$ for the group of interest versus LPA; $^{\dagger}P < 0.05$, $^{\dagger\dagger\dagger}P < 0.001$ for the group of interest versus IL6/sIL6R). LPA, Lysophosphatidic acid; hTM, Human trabecular meshwork; veh, Vehicle control; IL6, Interleukin-6; sIL6R, Soluble IL6 receptor; GAPDH, Glyceraldehyde 3-phosphate dehydrogenase; YAP, Yes-associated protein; pYAP, Phosphorylated YAP; TAZ, Transcriptional co-activator with a PDZ-binding motif; pTAZ, Phosphorylated TAZ; Pan-TEAD, Pan-transcriptional enhancer factor-domain; STAT3, Signal transducer and activator of transcription 3; pSTAT3, Phosphorylated STAT3; YAPi, YAP inhibitor.

overexpression of critical components of the actomyosin machinery, implicated in increased cell contractility and glaucoma.[18,19,29,62,63] We found that, in the absence of verteporfin, compared with veh, LPA, or IL6/sIL6R, or their interaction significantly overexpressed MLC2 ($P < 0.001$, respectively) in hTM cells; IL6/sIL6R alone or its interaction with LPA was markedly increased beyond LPA alone. However, in the presence of verteporfin, all the experimental groups showed a significant decrease in MLC2 ($P < 0.05$, respectively) in hTM cells relative to veh (Fig. 6A). Further, in the absence of verteporfin, RhoA was significantly upregulated by IL6/sIL6R alone or its interaction with LPA ($P < 0.001$ and $P < 0.01$, respectively) compared with veh. However, with verteporfin, veh, or LPA, or IL6/sIL6R significantly overexpressed RhoA ($P < 0.001$, respectively) in hTM cells, with no significant change by LPA + IL6/sIL6R (Fig. 6B). Finally, without verteporfin, LPA, or IL6/sIL6R, or their interaction markedly upregulated ROCK1 ($P < 0.001$, respectively) in hTM cells; LPA + IL6/sIL6R was profoundly heightened beyond either LPA alone or IL6/sIL6R alone. However, in the presence of verteporfin, all the experimental groups exhibited no significant differences in comparison with veh (Fig. 6C).

Verteporfin Repressed Increased Cell Contractility and Fibrotic ECM Proteins Induced by LPA and/or IL6 Trans-Signaling in hTM Cells

Next, we determined the causal role of verteporfin in LPA- and/or IL6 trans-signaling–mediated overexpression of α-SMA and key target ECM proteins. We observed that, in the

Investigative Ophthalmology & Visual Science

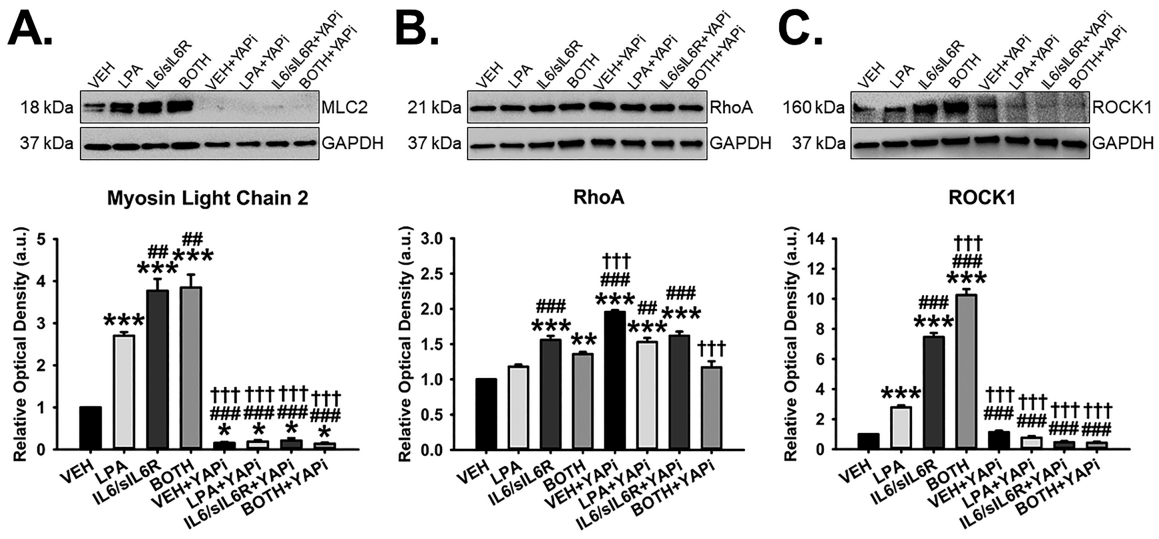

Figure 6. Verteporfin decreased LPA- and/or IL6 trans-signaling–mediated overexpression of key components of the actomyosin machinery in hTM cells. Primary hTM cells were cultured to confluency in complete medium, serum starved for 24 hours, and then treated with veh, LPA (20 µM), IL6 (100 ng/mL)/sIL6R (200 ng/mL), or both (LPA + IL6/sIL6R) for 24 hours with or without 2 µM verteporfin (a YAP inhibitor). Protein was extracted for Western blot analysis. GAPDH was used as an internal control for protein normalization. Representative blot (*top*) and densitometric analysis (*bottom*) of (**A**) MLC2, (**B**) RhoA, and (**C**) ROCK1. Columns and error bars are the means and standard error of mean (SEM). One-way ANOVA with the Tukey pairwise comparisons post hoc test was used for statistical analysis. ($n = 3$ biological replicates; $^{*}P < 0.05$, $^{**}P < 0.01$, $^{***}P < 0.001$ for the group of interest versus veh; $^{\#\#}P < 0.01$, $^{\#\#\#}P < 0.001$ for the group of interest versus LPA; $^{\dagger\dagger\dagger}P < 0.001$ for the group of interest versus IL6/sIL6R). LPA, Lysophosphatidic acid; hTM, Human trabecular meshwork; veh, Vehicle control; IL6, Interleukin-6; sIL6R, Soluble IL6 receptor; GAPDH, Glyceraldehyde 3-phosphate dehydrogenase; MLC2, Myosin light chain 2; RhoA, Ras homolog family member A; ROCK1, Rho-associated coiled-coil protein kinase 1; YAPi, Yes-associated protein inhibitor.

absence of verteporfin, all the experimental groups significantly upregulated α-SMA in hTM cells relative to veh; LPA + IL6/sIL6R was markedly increased beyond LPA alone or IL6/sIL6R alone. However, in the presence of verteporfin, veh, or LPA, or its interaction with IL6/sIL6R significantly downregulated α-SMA ($P < 0.05$, $P < 0.01$, and $P < 0.001$, respectively) in hTM cells, with no effect by IL6/sIL6R alone (Fig. 7A). In addition, without verteporfin, all the experimental groups significantly increased collagen I ($P < 0.001$, respectively) in hTM cells compared with veh. However, in the presence of verteporfin, collagen I was significantly decreased by all the experimental groups ($P < 0.001$, respectively) (Fig. 7B).

Further, fibronectin was significantly overexpressed by LPA, or IL6/sIL6R, or their interaction ($P < 0.001$, respectively) in hTM cells relative to veh in the absence of verteporfin; IL6/sIL6R alone was markedly increased beyond LPA alone or LPA + IL6/sIL6R. However, in the presence of verteporfin, all the experimental groups significantly downregulated fibronectin ($P < 0.001$, respectively) in hTM cells (Fig. 7C). Moreover, in the absence of verteporfin, LPA, or IL6/sIL6R, or their interaction significantly overexpressed laminin ($P < 0.001$) in hTM cells; LPA + IL6/sIL6R was further heightened beyond LPA alone or IL6/sIL6R alone. But, with verteporfin, laminin was markedly reduced among all the experimental groups ($P < 0.001$, respectively) (Fig. 7D). Also, in the absence of verteporfin, all the experimental groups markedly increased CYR61 ($P < 0.001$, respectively) in hTM cells relative to veh. However, in the presence of verteporfin, CYR61 was significantly decreased among veh, LPA, or IL6/ sIL6R ($P < 0.05$, $P < 0.01$, and $P < 0.01$, respectively), whereas LPA + IL6/sIL6R was not any different from veh (without verteporfin) (Fig. 7E). Finally, without verteporfin, compared with veh, all the experimental groups significantly overexpressed CTGF in hTM cells; LPA + IL6/sIL6R was more pronounced than LPA alone or IL6/sIL6R alone. However, in the presence of verteporfin, LPA- and/or IL6/sIL6R-induced expression of CTGF was not any different from veh (without verteporfin) (Fig. 7F).

The STAT3 Inhibitor Differentially Modulated Signaling Mediators of STAT3 and YAP/TAZ Pathways Induced by LPA and/or IL6 Trans-Signaling in hTM Cells

Next, before determining the definitive role of STAT3 in LPA- and/or IL6 trans-signaling–mediated ocular hypertensive phenotypes in hTM cells, we first determined the effect of the STAT3 inhibitor on LPA- and/or trans-signaling–induced protein increases of signaling mediators of STAT3 and YAP/TAZ pathways. We discovered that, without the STAT3 inhibitor, compared with veh, STAT3 was significantly upregulated by IL6/sIL6R alone or its interaction with LPA ($P < 0.001$, respectively) in hTM cells; LPA + IL6/sIL6R was profoundly increased beyond IL6/sIL6R alone or LPA alone, which saw no significant change. Similarly, in the presence of the STAT3 inhibitor, all the experimental groups markedly increased STAT3 ($P < 0.001$, respectively) in hTM cells relative to veh (without the inhibitor); almost all of these increases were beyond their respective counterparts in the absence of the STAT3 inhibitor (Fig. 8A).

In addition, without the STAT3 inhibitor, LPA, or IL6/sIL6R, or their interaction significantly increased pSTAT3 ($P < 0.01$, $P < 0.001$, and $P < 0.001$, respectively) in hTM cells; the increase by LPA + IL6/sIL6R was heightened

Investigative Ophthalmology & Visual Science

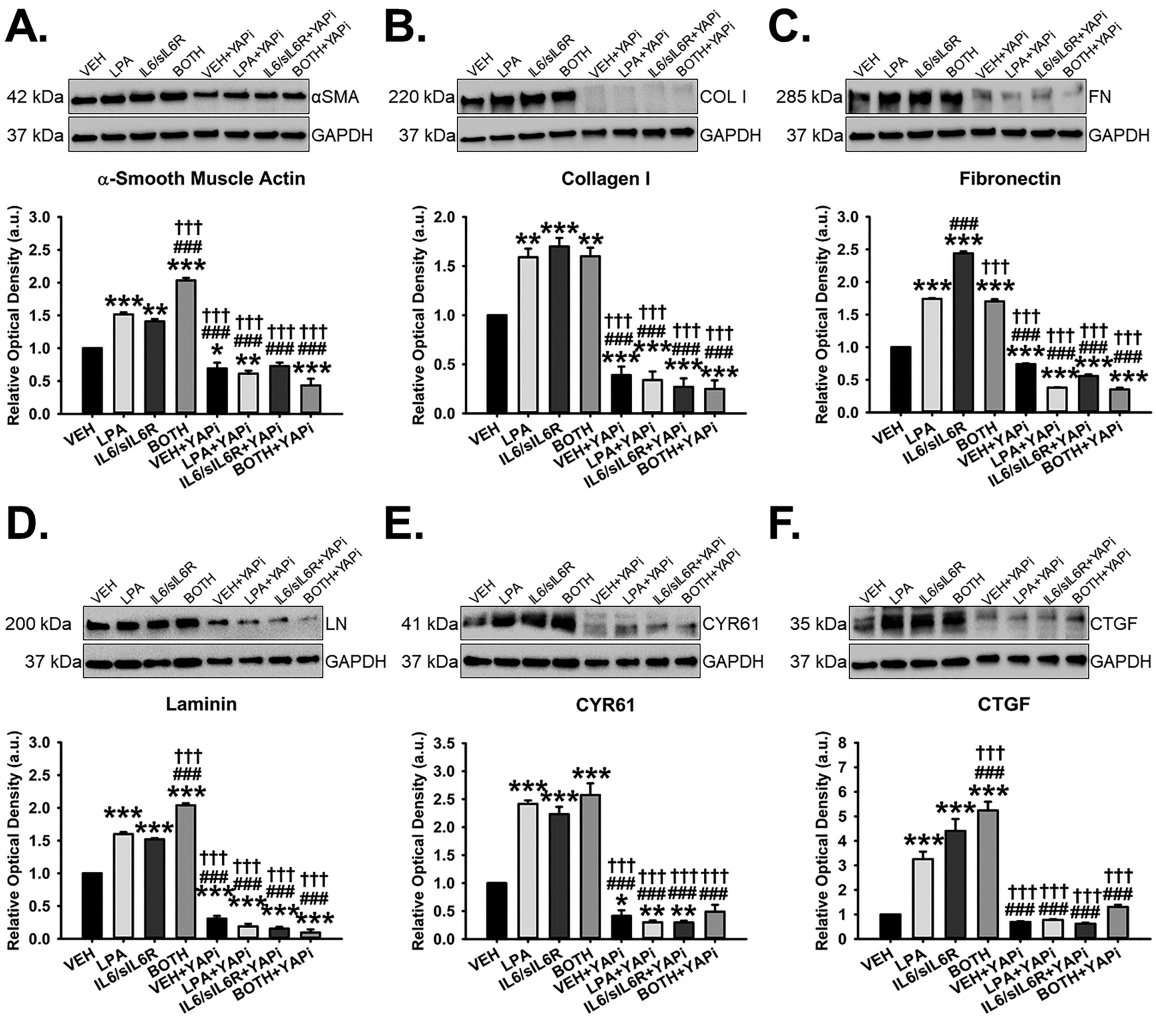

Figure 7. Verteporfin downregulated LPA- and/or IL6 trans-signaling–induced upregulation of cell contractility and fibrotic target ECM proteins in hTM cells. Primary hTM cells were cultured to confluency in complete medium, serum starved for 24 hours, and then treated with veh, LPA (20 μM), IL6 (100 ng/mL)/sIL6R (200 ng/mL), or both (LPA + IL6/sIL6R) in the presence or absence of 2 μM verteporfin (YAP inhibitor) for 24 hours. Protein was extracted for Western blotting. GAPDH was used as a housekeeping protein for normalization. Representative blot (*top*) and densitometric analysis (*bottom*) of (**A**) α-Smooth Muscle Actin, (**B**) Collagen I, (**C**) Fibronectin, (**D**) Laminin, (**E**) CYR61, and (**F**) CTGF. Columns and error bars are the means and standard error of mean (SEM). One-way ANOVA with the Tukey pairwise comparisons post hoc test was used for statistical analysis. ($n = 3$ biological replicates; $^{*}P < 0.05$, $^{**}P < 0.01$, $^{***}P < 0.001$ for the group of interest versus veh; $^{\#\#\#}P < 0.001$ for the group of interest versus LPA; $^{\dagger\dagger\dagger}P < 0.001$ for the group of interest versus IL6/sIL6R). LPA, Lysophosphatidic acid; hTM, Human trabecular meshwork; veh, Vehicle control; IL6, Interleukin-6; sIL6R, Soluble IL6 receptor; GAPDH, Glyceraldehyde 3-phosphate dehydrogenase; CYR61, Cysteine-rich angiogenic inducer 61; CTGF, Connective tissue growth factor; YAPi, Yes-associated protein inhibitor.

beyond LPA alone or IL6/sIL6R alone. In the presence of the STAT3 inhibitor, whereas veh and LPA alone was not any different from veh (without the inhibitor), IL6/sIL6R alone or its interaction with LPA significantly increased pSTAT3 in hTM cells, although these increases were significantly lower than their respective counterparts in the absence of the STAT3 inhibitor (Fig. 8B). Further, without the STAT3 inhibitor, compared with veh, LPA, or IL6/sIL6R, or their interaction markedly overexpressed YAP ($P < 0.01$, $P < 0.001$, and $P < 0.001$, respectively) in hTM cells; with LPA + IL6/sIL6R being further overexpressed beyond LPA alone or IL6/sIL6R alone.

With the STAT3 inhibitor, YAP was significantly decreased among all the experimental groups ($P < 0.001$, respectively), except LPA + IL6/sIL6R, which saw no significant change relative to veh (without the inhibitor) (Fig. 8C). Moreover, regardless of the STAT3 inhibitor, all the experimental groups significantly overexpressed pYAP ($P < 0.001$, respectively) in hTM cells relative to veh (without the inhibitor) (Fig. 8D). Also, in the absence of the STAT3 inhibitor, TAZ was significantly increased by IL6/sIL6R alone or its interaction with LPA relative to veh. However, with the STAT3 inhibitor, surprisingly, TAZ was profoundly and significantly overexpressed by all the experimental groups ($P < 0.001$, respectively) in hTM cells; these increases were way beyond their respective counterparts in the absence of the STAT3 inhibitor, including IL6/sIL6 or LPA + IL6/sIL6R (Fig. 8E).

Furthermore, in the absence of the STAT3 inhibitor, only IL6/sIL6R alone or its interaction with LPA markedly upregulated pTAZ in hTM cells compared with veh; LPA + IL6/sIL6R

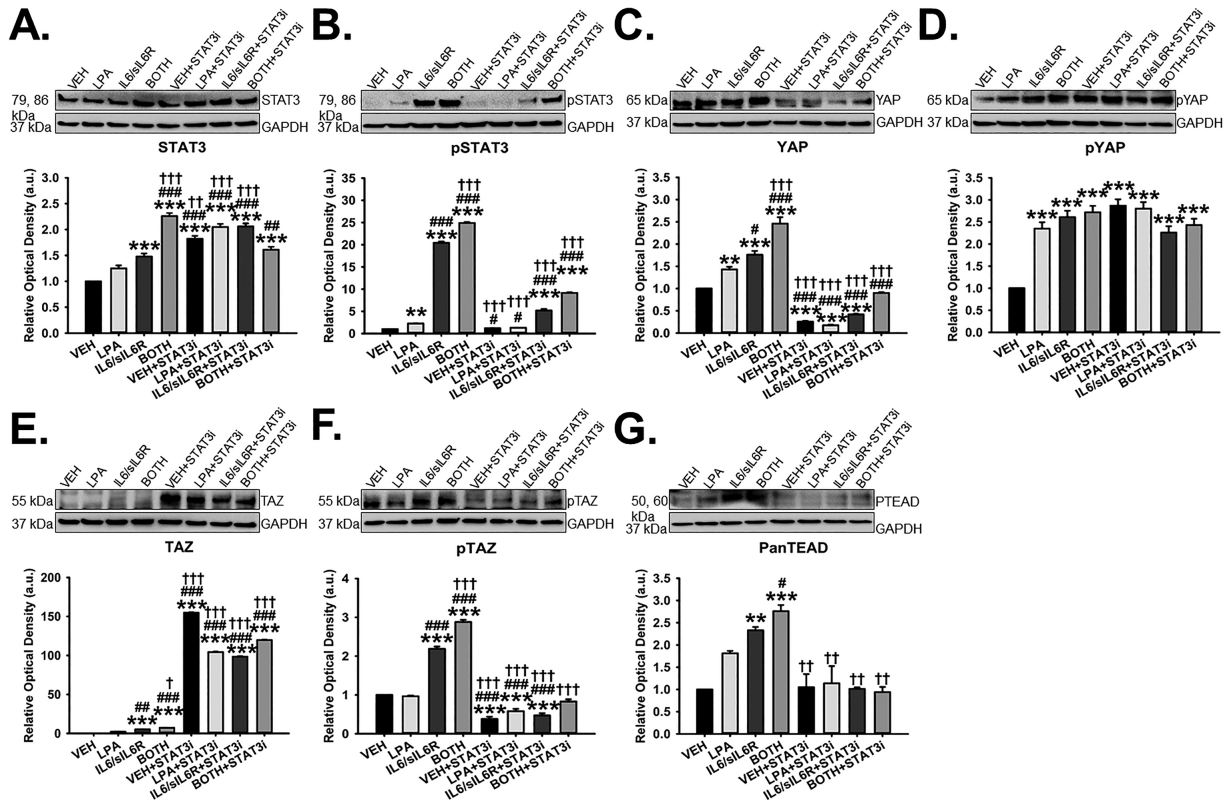

Figure 8. The STAT3 inhibitor differentially modulated LPA- and/or IL6 trans-signaling–mediated overexpression of signaling mediators of STAT3 and YAP/TAZ in hTM cells. Primary hTM cells were cultured to confluency in complete medium, serum starved for 24 hours, and then treated with veh, LPA (20 µM), IL6 (100 ng/mL)/sIL6R (200 ng/mL), or both (LPA + IL6/sIL6R) in the presence or absence of 2 µM STAT3 inhibitor for 24 hours. Protein was isolated for Western blot analysis. GAPDH was used as an internal control for protein normalization. Representative blot (*top*) and densitometric analysis (*bottom*) of (**A**) YAP, (**B**) pYAP, (**C**) TAZ, (**D**) pTAZ, (**E**) Pan-TEAD, (**F**) STAT3, and (**G**) pSTAT3. Columns and error bars are the means and standard error of mean (SEM). One-way ANOVA with the Tukey pairwise comparisons post hoc test was used for statistical analysis. ($n = 3$ biological replicates; $^{**}P < 0.01$, $^{***}P < 0.001$ for the group of interest versus veh; $^{\#}P < 0.05$, $^{\#\#}P < 0.01$, $^{\#\#\#}P < 0.001$ for the group of interest versus LPA; $^{\dagger\dagger}P < 0.01$, $^{\dagger\dagger\dagger}P < 0.001$ for the group of interest versus IL6/sIL6R). LPA, Lysophosphatidic acid; hTM, Human trabecular meshwork; veh, Vehicle control; IL6, Interleukin-6; sIL6R, Soluble IL6 receptor; GAPDH, Glyceraldehyde 3-phosphate dehydrogenase; YAP, Yes-associated protein; pYAP, Phosphorylated YAP; TAZ, Transcriptional co-activator with a PDZ-binding motif; pTAZ, Phosphorylated TAZ; Pan-TEAD, Pan-transcriptional enhancer factor-domain; STAT3, Signal transducer and activator of transcription 3; pSTAT3, Phosphorylated STAT3; STAT3i, STAT3 inhibitor.

was more pronounced than IL6/sIL6R alone. However, in the presence of the STAT3 inhibitor, pTAZ was significantly decreased by all the experimental groups ($P < 0.001$, respectively) except LPA + IL6/sIL6, which showed no difference (Fig. 8F). Finally, in the absence of the STAT3 inhibitor, Pan-TEAD was increased by LPA, or IL6/sIL6R alone, or LPA + IL6/sIL6R; with the latter two reaching significance ($P < 0.01$ and $P < 0.001$, respectively). However, in the presence of the STAT3 inhibitor, all the experimental groups showed no marked differences in Pan-TEAD in hTM cells relative to veh (without the inhibitor) (Fig. 8G).

The STAT3 Inhibitor Differentially Regulated Crucial Components of the Actomyosin Machinery Induced by LPA and/or IL6 Trans-Signaling in hTM Cells

After confirming/determining the inhibitory effects of the STAT3 inhibitor on the protein expression of signaling molecules of STAT3 and YAP/TAZ pathways, next, we determined the causal role of this inhibitor in LPA- and/or IL6 trans-signaling–mediated overexpression of key components of the actomyosin machinery. We discovered that, in the absence of the STAT3 inhibitor, MLC2 was markedly increased among all the experimental groups ($P < 0.001$, respectively) in hTM cells relative to veh; and LPA + sIL6R was increased beyond that of LPA alone. However, in the presence of the STAT3 inhibitor, whereas veh or IL6/sIL6R alone had no significant impact on MLC2, LPA alone or LPA + IL6/sIL6R markedly increased its expression ($P < 0.001$, respectively) in hTM cells (Fig. 9A). Similarly, in the absence of the STAT3 inhibitor, all the experimental groups markedly overexpressed RhoA in hTM cells compared with veh; LPA + IL6/sIL6 was more pronounced than either LPA alone or IL6/sIL6R alone. However, in the presence of the STAT3 inhibitor, whereas veh significantly increased RhoA ($P < 0.001$) in hTM cells, all the other experimental groups were not any different in relation to veh (without the inhibitor) (Fig. 9B).

Finally, in the absence of the STAT3 inhibitor, all the experimental groups significantly increased ROCK1

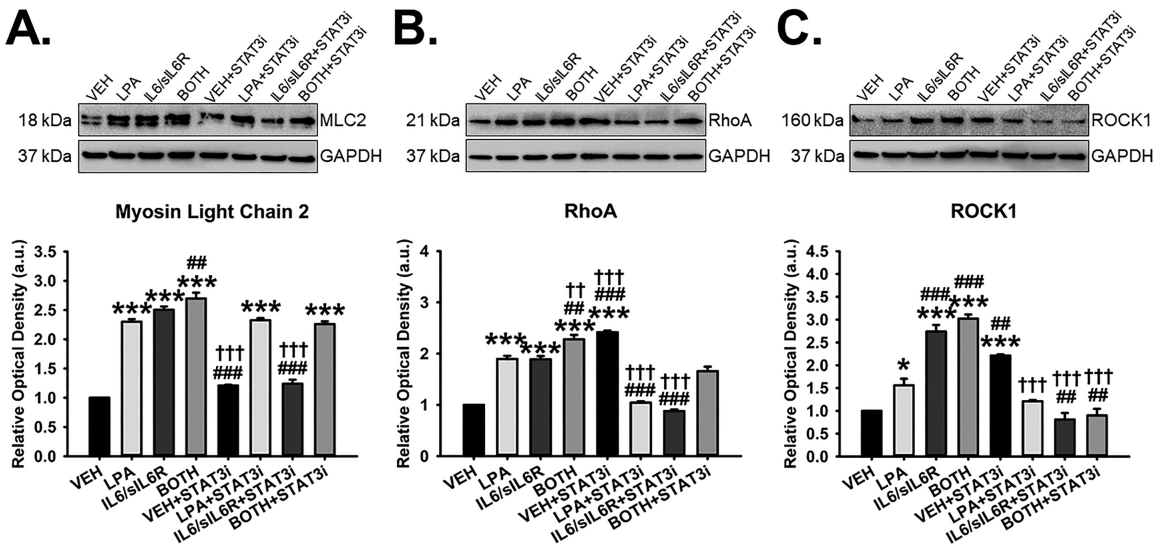

Figure 9. The STAT3 inhibitor differentially regulated LPA- and/or IL6 trans-signaling–induced overexpression of key components of the actomyosin machinery in hTM cells. Primary hTM cells were cultured to confluency in complete medium, serum starved for 24 hours, and then treated with veh, LPA (20 µM), IL6 (100 ng/mL)/sIL6R (200 ng/mL), or both (LPA + IL6/sIL6R) for 24 hours with or without 2 µM STAT3 inhibitor. Protein was extracted for Western blot analysis. GAPDH was used as a housekeeping protein for normalization. Representative blot (*top*) and densitometric analysis (*bottom*) of (**A**) MLC2, (**B**) RhoA, and (**C**) ROCK1. Columns and error bars are the means and standard error of mean (SEM). One-way ANOVA with the Tukey pairwise comparisons post hoc test was used for statistical analysis. (n = 3 biological replicates; $^{*}P < 0.05$, $^{***}P < 0.001$ for the group of interest versus veh; $^{\#\#}P < 0.01$, $^{\#\#\#}P < 0.001$ for the group of interest versus LPA; $^{\dagger\dagger}P < 0.01$, $^{\dagger\dagger\dagger}P < 0.001$ for the group of interest versus IL6/sIL6R). LPA, Lysophosphatidic acid; hTM, Human trabecular meshwork; veh, Vehicle control; IL6, Interleukin-6; sIL6R, Soluble IL6 receptor; GAPDH, Glyceraldehyde 3-phosphate dehydrogenase; MLC2, Myosin light chain 2; RhoA, Ras homolog family member A; ROCK1, Rho-associated coiled-coil protein kinase 1; STAT3, Signal transducer and activator of transcription 3; STAT3i, STAT3 inhibitor.

($P < 0.001$, respectively) in hTM cells; IL6/sIL6 alone or LPA + IL6/sIL6R was further heightened beyond LPA alone. However, in the presence of the STAT3 inhibitor, only veh significantly upregulated ROCK1 ($P < 0.001$) in hTM cells, with all the other experimental groups showing on difference in comparison with veh (without the inhibitor) (Fig. 9C).

The STAT3 Inhibitor Differentially Modulated Increased Cell Contractility and Fibrotic ECM Proteins Induced by LPA and/or IL6 Trans-Signaling in hTM Cells

Finally, we determined the causal role of the STAT3 inhibitor in LPA- and/or IL6 trans-signaling–induced overexpression of α-SMA and crucial target ECM proteins in hTM cells. We found that, in the absence of the STAT3 inhibitor, compared with veh, all the experimental groups markedly overexpressed α-SMA ($P < 0.001$, respectively) in hTM cells; LPA + IL6/sIL6R was more pronounced than either LPA alone or IL6/sIL6R alone. In the presence of the STAT3 inhibitor, all the experimental groups significantly increased α-SMA ($P < 0.001$, respectively) in hTM cells relative to veh (without the inhibitor); however, these increases in α-SMA were markedly lower ($P < 0.001$, respectively) compared with the observations in the respective groups in the absence of the STAT3 inhibitor (Fig. 10A).

Additionally, in the absence of the STAT3 inhibitor, compared with veh, all the experimental groups markedly overexpressed collagen I ($P < 0.001$, respectively) in hTM cells; LPA + IL6/sIL6R was further heightened beyond LPA alone or IL6/sIL6R alone. However, with the STAT3 inhibitor, as expected, all the experimental groups significantly downregulated collagen I ($P < 0.001$, respectively) in hTM cells relative to veh (without the inhibitor) (Fig. 10B). Further, in the absence of the STAT3 inhibitor, IL6/sIL6R or its interaction with LPA markedly upregulated fibronectin ($P < 0.001$, respectively) in hTM cells compared with veh. However, in the presence of the STAT3 inhibitor, unexpectedly, all the experimental groups further heightened fibronectin's expression in hTM cells relative to veh or their respective counterparts in the absence of the inhibitor (Fig. 10C).

Similarly, without the STAT3 inhibitor, all the experimental groups significantly overexpressed laminin ($P < 0.001$, respectively) in hTM cells compared with veh; LPA + IL6/sIL6R was more pronounced than either LPA alone or IL6/sIL6R alone. However, in the presence of the STAT3 inhibitor, all the experimental groups again surprisingly further overexpressed laminin ($P < 0.001$, respectively) in hTM cells relative to veh or their respective groups in the absence of the inhibitor (Fig. 10D). Moreover, without the STAT3 inhibitor, compared with veh, all the experimental groups markedly increased CYR61 in hTM cells; LPA + IL6/sIL6R was more pronounced beyond LPA alone or IL6/sIL6R alone. However, in the presence of the STAT3 inhibitor, all the experimental groups except IL6/sIL6R further increased CYR61 ($P < 0.001$, respectively) in hTM cells compared with veh or their respective groups in the absence of the inhibitor (Fig. 10E).

Likewise, in the absence of the STAT3 inhibitor, compared with veh, all the experimental groups significantly overexpressed CTGF ($P < 0.001$, respectively) in hTM cells; LPA + IL6/sIL6R was heightened beyond LPA alone. However, in the presence of the STAT3 inhibitor, all the experimental groups significantly further overexpressed CTGF ($P < 0.001$,

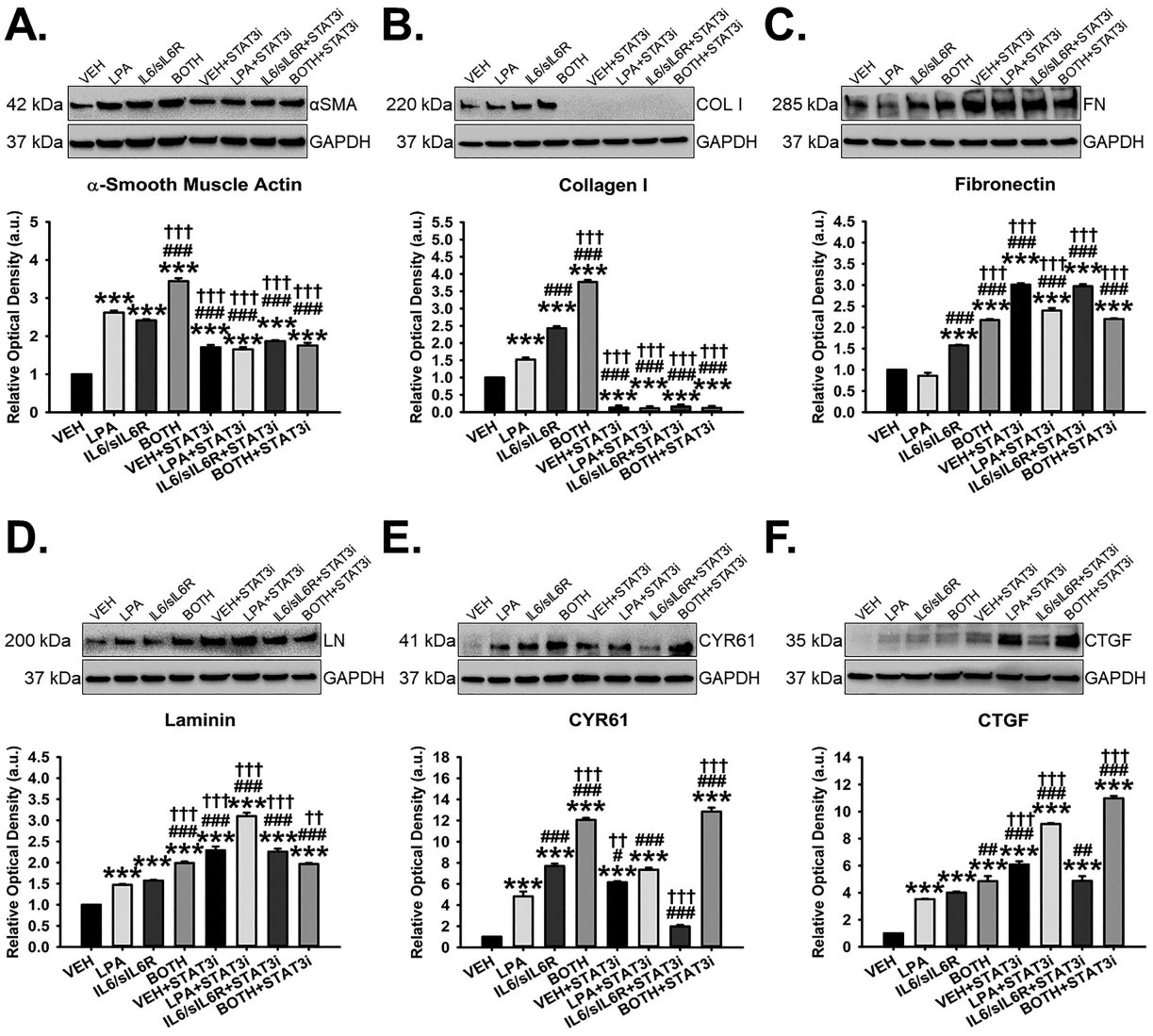

Figure 10. The STAT3 inhibitor differentially modulated LPA- and/or IL6 trans-signaling–mediated increase of cell contractility and target ECM proteins in hTM cells. Primary hTM cells were cultured to confluency in complete medium, serum starved for 24 hours, and then treated with veh, LPA (20 µM), IL6 (100 ng/mL)/sIL6R (200 ng/mL), or both (LPA + IL6/sIL6R) for 24 hours in the presence or absence of 2 µM STAT3 inhibitor. Protein was extracted for Western blotting. GAPDH was used as an internal control for protein normalization. Representative blot (*top*) and densitometric analysis (*bottom*) of (**A**) α-Smooth Muscle Actin, (**B**) Collagen I, (**C**) Fibronectin, (**D**) Laminin, (**E**) CYR61, and (**F**) CTGF. Columns and error bars are the means and standard error of mean (SEM). One-way ANOVA with the Tukey pairwise comparisons post hoc test was used for statistical analysis. ($n = 3$ biological replicates; $^{***}P < 0.001$ for the group of interest versus veh; $^{\#\#}P < 0.01$, $^{\#\#\#}P < 0.001$ for the group of interest versus LPA; $^{\dagger\dagger}P < 0.01$, $^{\dagger\dagger\dagger}P < 0.001$ for the group of interest versus IL6/sIL6R). ECM, Extracellular matrix; LPA, Lysophosphatidic acid; hTM, Human trabecular meshwork; veh, Vehicle control; IL6, Interleukin-6; sIL6R, Soluble IL6 receptor; GAPDH, Glyceraldehyde 3-phosphate dehydrogenase; CYR61, Cysteine-rich angiogenic inducer 61; CTGF, Connective tissue growth factor; STAT3, Signal transducer and activator of transcription 3; STAT3i, STAT3 inhibitor.

respectively) in hTM cells relative to veh or their respective counterparts in the absence of the inhibitor (Fig. 10F).

Discussion

One of the major factors implicated in the pathobiology of the TM associated with increased restriction to aqueous humor and elevated IOP in POAG is aberrant remodeling of the ECM.[13,14,21,64–66] As a part of its diverse normal homeostatic functions, the ECM regulates and sequesters growth or bioactive factors from the extracellular milieu.[67,68] However, this ECM-dependent regulation and sequestration of bioactive factors is impaired in the event of aberrant ECM remodeling. One of the major consequences of this ECM dyshomeostasis is increased levels of growth or bioactive factors in the extracellular milieu associated with their dysregulated cell signaling pathways.[67,68] These aberrant signaling pathways are typically interconnected and hardly independent of one another.[24,32,69,70] Therefore, determining downstream targets on which these pathways converge may enhance effective and efficient blockade of attendant/accompanying fibrotic phenotypes associated with elevated IOP. Consequently, in this study, for the first time, we show that LPA, which is elevated in the aqueous humor of patients with POAG,[40] and IL6 trans-signaling (relevant because sIL6R is elevated in the aqueous humor of patients with POAG

Investigative Ophthalmology & Visual Science

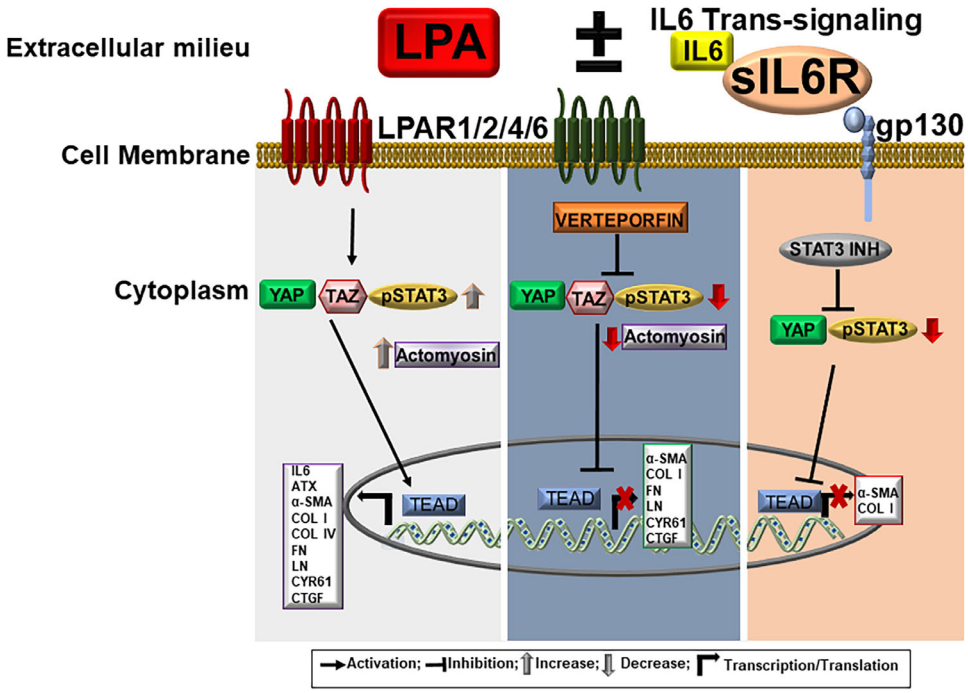

Figure 11. Summary of LPA and/or IL6 trans-signaling–mediated fibrotic phenotypes in hTM cells and inhibitory outcomes. (***Left cellular compartment***) LPA and/or IL6 trans-signaling–activated YAP, TAZ and STAT3, overexpressed key components of the actomyosin machinery, in correlation with increased expression of specific receptors and ligands, α-SMA and fibrotic ECM genes/proteins in hTM cells. (***Middle cellular compartment***) Verteporfin abrogated LPA and/or IL6 trans-signaling–mediated activation of YAP, TAZ, and STAT3, overexpression of critical components of the actomyosin machinery, associated with upregulation of α-SMA and target ECM proteins in hTM cells. (***Right cellular compartment***) A STAT3 inhibitor attenuated LPA and/or IL6 trans-signaling–induced activation of YAP and STAT3 associated with overexpression of α-SMA and collagen I in hTM cells. LPA, Lysophosphatidic acid; COL I, Collagen I; COL IV, Collagen IV; FN, Fibronectin; LN, Laminin; LPAR, LPA receptor; IL6, Interleukin-6; sIL6R, Soluble IL6 receptor; gp130, Glycoprotein 130; YAP, Yes-associated protein; pSTAT3, Phosphorylated STAT3; STAT3, Signal transducer and activator of transcription; STAT3i or STAT3 INH, STAT3 inhibitor; ATX, Autotaxin; α-SMA, α-Smooth muscle actin; TAZ, Transcriptional coactivator with a PDZ-binding motif; TEAD, Transcriptional enhancer factor domain; CYR61, Cysteine-rich angiogenic inducer 61; CTGF, Connective tissue growth factor.

as well)[32] interact via YAP, TAZ, and pSTAT3 signaling molecules to precipitate ocular hypertensive phenotypes in hTM cells (Fig. 11; left cellular compartment).

Specifically, although there were some slight variations, overall, this LPA-IL6/sIL6 interaction resulted in increases in specific receptors/ligands (e.g., *gp130*, *IL6*, and *ATX*) and fibrotic changes such as overexpression of key components of the actomyosin machinery (e.g., MLC2, pMLC2, ROCK1, and F-actin), increased cell contractility (e.g., α-SMA), and increased deposition of ECM proteins/genes (e.g., collagen I, collagen IV, fibronectin, laminin, CYR61, and CTGF) in hTM cells. Respective changes induced by LPA alone or IL6 trans-signaling alone in hTM cells were mostly markedly less pronounced compared with their interaction (i.e., LPA + IL6/sIL6R), suggesting synergistic crosstalk. Further, we show that verteporfin (which is designated a YAP inhibitor) completely abrogated LPA- and/or IL6 trans-signaling–induced overexpression of all these aforementioned ocular hypertensive phenotypes relative to veh by inhibiting YAP, TAZ, and pSTAT3 (Fig. 11; middle cellular compartment). Finally, a STAT3 inhibitor, in contrast, partially or fully attenuated only few fibrotic phenotypes (e.g., collagen I and α-SMA) mediated by LPA and/or IL6 trans-signaling in hTM cells, by inhibiting pSTAT3 and YAP, but not TAZ (Fig. 11; right cellular compartment).

First, LPA alone or IL6 alone differentially modulated the gene expression of specific receptors and ligands. For instance, while LPA alone upregulated *LPAR1* and *LPAR4* genes, IL6 trans-signaling alone intriguingly overexpressed *LPAR2* and *LPAR6* genes. Because these receptors are mechanosensitive, perhaps, mechanically stretching hTM cells might have resulted in greater overexpression of LPARs[33] relative to that induced by LPA and/or IL6 trans-signaling in this study. However, the differential upregulation of *LPAR1*, *LPAR2*, *LPAR4*, and *LPAR6* genes in hTM cells in response to LPA alone or IL6 trans-signaling alone without any mechanical stretching, stamps their relevance in aqueous (dys)homeostasis. However, LPA + IL6 trans-signaling had no positive impact on the gene expression of LPARs in hTM cells. Instead, LPA + IL6 trans-signaling overexpressed the *gp130* gene associated with the upregulation of *IL6* or *ATX* genes in hTM cells. This observation may (1) suggest that the expression of IL6 receptors is more critical to establishing interaction between LPA and IL6, and (2) represent a probable feedforward mechanism to perpetuate fibrotic phenotypes synergistically mediated by LPA + IL6 trans-signaling.[71,72]

Second, LPA- and/or IL6 trans-signaling–dependent nuclear localization/overexpression of signaling mediators like YAP, TAZ, Pan-TEAD, and pSTAT3 implicates them as critical downstream regulatory nodes in target gene/protein expression. Regardless of the nuclear localization and/or upregulation of YAP, TAZ, or Pan-TEAD (suggesting activation of the YAP/TAZ pathway) in hTM cells, it is worth noting

that pYAP or pTAZ was unexpectedly also upregulated (suggesting inactivation of the YAP/TAZ pathway). However, consistent with our recent study[44] and others,[43] redundant experimental approaches (e.g., immunocytochemistry, Western blotting using whole cell lysates and subcellular fractionation, luciferase assays) may be critical to definitively determine whether transcriptional coactivators like YAP and TAZ are active or otherwise. Accompanying these changes in signaling mediators was overexpression of key components of the actomyosin machinery involved in aberrant contractile properties of hTM cells implicated in elevated IOP and glaucoma.[62,63,73] For instance, ROCK1 is the target of a relatively new class of IOP-lowering medications that inhibit increased contractility to "relax" noncompliant hTM cells.[10]

Furthermore, overexpression of intracellular and extracellular fibrotic phenotypes like α-SMA, collagens I and IV, fibronectin, laminin, CYR61, and CTGF implicated in endoplasmic reticulum (ER) stress, elevated IOP, and glaucoma[28,40,74–79] were observed. For instance, increased deposition of fibronectin is associated with ER stress,[76] and is necessary for the assembly/maturation of other ECM proteins like collagen IV, fibrillin and laminin,[15] which may contribute to altered tissue biomechanics.[20,21] Thus, the inhibition of fibronectin's fibrillogenesis ameliorates TGFβ2-induced elevated IOP in mice.[80] In addition, increased expression of collagen IV and laminin highlight the role of aberrant basement membrane changes in fibrotic phenotypes.[81–83] Moreover, CTGF is elevated in pseudoexfoliation glaucoma[27,84] and POAG[40] and its upregulation causes elevated IOP in mice.[28]

Third, consistent with previous studies,[57,58] verteporfin completely abolished LPA- and/or IL6 trans-signaling–mediated overexpression of the aforementioned ocular hypertensive phenotypes in hTM cells. We show that verteporfin did this by effectively attenuating LPA- and/or IL6 trans-signaling–dependent upregulation of not only YAP, TAZ and Pan-TEAD, but also pSTAT3. This suggests that (1) LPA and/or IL6 trans-signaling converge on crosstalk among these downstream signaling mediators, and (2) verteporfin may be an effective strategy of lowering IOP.[58] However, congruent with previous studies,[58] notably, verteporfin downregulated LPA- and/or IL6 trans-signaling–mediated overexpression of pYAP and pTAZ as well in hTM cells. Whereas this observation may suggest the inhibitory effect of verteporfin on YAP and TAZ in hTM cells was probably not effective, concurrent marked decreases in total YAP and total TAZ and their respective fibrotic target proteins convey a different message. As mentioned elsewhere in this article, this finding reinforces the need for redundant approaches to conclusively determine the activated/inactivated states of YAP and TAZ congruent with this and our previous study,[44] as well as other investigations.[43]

Finally, using a safe but effective dose, the STAT3 inhibitor partially or fully inhibited LPA- and/or IL6 trans-signaling–induced overexpression of only few fibrotic targets (e.g., α-SMA or collagen I), while paradoxically exaggerating the expression of few others (e.g., fibronectin or laminin) in hTM cells. The reason for this observation was that, unlike verteporfin, the STAT3 inhibitor inhibited pSTAT3, YAP and Pan-TEAD, but not TAZ. This suggests that (1) the functions of YAP and TAZ are not necessarily interchangeable consistent with previous studies,[57,85–87] (2) TAZ and/or other IL6 trans-signaling pathways (e.g., MAPK or PI3/Akt pathways)[50,88] most likely drove overexpression of fibrotic targets despite the STAT3 inhibitor, independent of Pan-TEAD, and (3) the nature of interaction between IL6 trans-signaling and other signaling pathways via pSTAT3 may be target protein- and/or signaling pathway-dependent in agreement with a previous study.[32]

In conclusion, here, we provide the first report on synergistic crosstalk between LPA and IL6 trans-signaling via mechanotransducers, YAP and TAZ, and the active form of STAT3 (pSTAT3) in hTM cells. By completely inhibiting YAP, TAZ, Pan-TEAD, and pSTAT3, verteporfin may be an effective therapeutic for ameliorating LPA and/or IL6 trans-signaling–mediated overexpression of ocular hypertensive phenotypes in hTM cells.

Acknowledgments

The authors thank their funding sources: student Vision Research Support Grant at University of Houston College of Optometry (UHCO) (F.Y.), startup funding at UHCO (V.K.R.), National Institute of Health grants 1R01EY026048 (V.K.R.), and 5 P30 EY007551-30 (NEI Core grant to UHCO). Finally, we would like to thank the organ donors and SavingSight (Kansas City, MO) eye bank for the donor tissues used in this study.

Supported by student Vision Research Support Grant (sVRSG), University of Houston College of Optometry (UHCO) (F.Y.), NIH/NEI grants EY026048-01A1 (V.K.R.), startup funding from UHCO (V.K.R.), and 5 P30 EY007551-30 (NEI Core grant to UHCO).

Disclosure: **F. Yemanyi**, None; **V. Raghunathan**, None

References

1. Quigley HA. Number of people with glaucoma worldwide. *Br J Ophthalmol*. 1996;80(5):389–393.
2. Kapetanakis VV, Chan MPY, Foster PJ, Cook DG, Owen CG, Rudnicka AR. Global variations and time trends in the prevalence of primary open angle glaucoma (POAG): a systematic review and meta-analysis. *Br J Ophthalmol*. 2016;100(1):86–93.
3. Gupta P, Zhao D, Guallar E, Ko F, Boland M V., Friedman DS. Prevalence of glaucoma in the united states: the 2005–2008 national health and nutrition examination survey. *Investig Ophthalmol Vis Sci*. 2016;57(6):2905–2913.
4. Tham YC, Li X, Wong TY, Quigley HA, Aung T, Cheng CY. Global prevalence of glaucoma and projections of glaucoma burden through 2040: a systematic review and meta-analysis. *Ophthalmology*. 2014;121(11):2081–2090.
5. Heijl A, Leske MC, Bengtsson B, Hyman L, Bengtsson B, Hussein M. Reduction of intraocular pressure and glaucoma progression. *Arch Ophthalmol*. 2002;120:1268–1279.
6. Acott TS, Kelley MJ. Extracellular matrix in the trabecular meshwork. *Exp Eye Res*. 2008;86(4):543–561.
7. Vranka JA, Kelley MJ, Acott TS, Keller KE. Extracellular matrix in the trabecular meshwork: intraocular pressure regulation and dysregulation in glaucoma. *Exp Eye Res*. 2015;133:112–125.
8. Stamer WD, Acott TS. Current understanding of conventional outflow dysfunction in glaucoma. *Curr Opin Ophthalmol*. 2012;23(2):135–143.
9. Rohen J, Lutjen-Drecoll E, Flugel C, Meyer M, Grierson I. Ultrastructure of the trabecular meshwork in untreated cases of POAG.pdf. *Exp Eye Res*. 1993;56:683–692.
10. Ren R, Li G, Le TD, Kopczynski C, Stamer WD. Netarsudil increases outflow facility in human eyes through multiple mechanisms. *Investig Ophthalmol Vis Sci*. 2016;57(14):6197–6209.

11. Kaufman PL, Kaufman PL. Expert opinion on pharmacotherapy latanoprostene bunod ophthalmic solution 0.024 % for IOP lowering in glaucoma and ocular hypertension and ocular hypertension. *Expert Opin Pharmacother*. 2017;18(4):433–444.
12. Flügel-Koch C, Ohlmann A, Fuchshofer R, Welge-Lüssen U, Tamm ER. Thrombospondin-1 in the trabecular meshwork: localization in normal and glaucomatous eyes, and induction by TGF-β1 and dexamethasone in vitro. *Exp Eye Res*. 2004;79(5):649–663.
13. Rohen JW, Futa R, Liitjen-Drecoll E. The fine structure of the cribriform meshwork in normal and glaucomatous eyes as seen in tangential sections. *Investig Ophthalmol Vis Sci*. 1981;21:574–585.
14. Medina-Ortiz WE, Belmares R, Neubauer S, Wordinger RJ, Clark AF. Cellular fibronectin expression in human trabecular meshwork and induction by transforming growth factor-β2. *Investig Ophthalmol Vis Sci*. 2013;54(10):6779–6788.
15. Filla MS, Dimeo KD, Tong T, Peters DM. Disruption of fibronectin matrix affects type IV collagen, fibrillin and laminin deposition into extracellular matrix of human trabecular meshwork (HTM) cells. *Exp Eye Res*. 2017;165:7–19.
16. Lütjen-Drecoll E, Rittig M, Rauterberg J, Jander R, Mollenhauer J. Immunomicroscopical study of type VI collagen in the trabecular meshwork of normal and glaucomatous eyes. *Exp Eye Res*. 1989;48(1):139–147.
17. Yemanyi F, Vranka J, Raghunathan VK. Glucocorticoid-induced cell-derived matrix modulates transforming growth factor β2 signaling in human trabecular meshwork cells. *Sci Rep*. 2020;10(1):15641.
18. Clark AF, Miggans ST, Wilson K, Browder S, McCartney MD. Cytoskeletal changes in cultured human glaucoma trabecular meshwork cells. *J Glaucoma*. 1995;4(3):183–188.
19. Hoare MJ, Grierson I, Brotchie D, Pollock N, Cracknell K, Clark AF. Cross-linked actin networks (CLANs) in the trabecular meshwork of the normal and glaucomatous human eye in situ. *Investig Ophthalmol Vis Sci*. 2009;50(3):1255–1263.
20. Last JA, Pan T, Ding Y, et al. Elastic modulus determination of normal and glaucomatous human trabecular meshwork. *Investig Ophthalmol Vis Sci*. 2011;52(5):2147–2152.
21. Wang K, Li G, Read AT, et al. The relationship between outflow resistance and trabecular meshwork stiffness in mice. *Sci Rep*. 2018;8(1):5848.
22. Wang WH, McNatt LG, Pang IH, et al. Increased expression of the WNT antagonist sFRP-1 in glaucoma elevates intraocular pressure. *J Clin Invest*. 2008;118(3):1056–1064.
23. Agarwal P, Daher AM, Agarwal R. Aqueous humor TGF-β2 levels in patients with open-angle glaucoma: a meta-analysis. *Mol Vis*. 2015;21:612–620.
24. Webber HC, Bermudez JY, Sethi A, Clark AF, Mao W. Crosstalk between TGFβ and Wnt signaling pathways in the human trabecular meshwork. *Exp Eye Res*. 2016;148:97–102.
25. Tripathi RC, Chan WFA, Li J, Tripathi BJ. Trabecular cells express the TGF-β2 gene and secrete the cytokine. *Exp Eye Res*. 1994;58(5):523–528.
26. Sethi A, Wordinger RJ, Clark AF. Gremlin utilizes canonical and non-canonical TGF b signaling to induce lysyl oxidase (LOX) genes in human trabecular meshwork cells q. *Exp Eye Res*. 2013;113:117–127.
27. Browne JG, Ho SL, Kane R, et al. Connective tissue growth factor is increased in pseudoexfoliation glaucoma. *Investig Ophthalmol Vis Sci*. 2011;52(6):3660–3666.
28. Junglas B, Kuespert S, Seleem AA, et al. Connective tissue growth factor causes glaucoma by modifying the actin cytoskeleton of the trabecular meshwork. *Am J Pathol*. 2012;180(6):2386–2403.
29. Mettu PS, Deng PF, Misra UK, Gawdi G, Epstein DL, Rao PV. Role of lysophospholipid growth factors in the modulation of aqueous humor outflow facility. *Investig Ophthalmol Vis Sci*. 2004;45(7):2263–2271.
30. Iyer P, Lalane R, Morris C, Challa P, Vann R, Rao PV. Autotaxin-lysophosphatidic acid axis is a novel molecular target for lowering intraocular pressure. *PLoS One*. 2012;7(8):e42627.
31. Honjo M, Igarashi N, Nishida J, et al. Role of the autotaxin-LPA pathway in dexamethasone-induced fibrotic responses and extracellular matrix production in human trabecular meshwork cells. *Investig Ophthalmol Vis Sci*. 2018;59(1):21–30.
32. Inoue-Mochita M, Inoue T, Kojima S, et al. Interleukin-6–mediated trans-signaling inhibits transforming growth factor-β signaling in trabecular meshwork cells. *J Biol Chem*. 2018;293(28):10975–10984.
33. Ho LTY, Skiba N, Ullmer C, Rao PV. Lysophosphatidic acid induces ECM production via activation of the mechanosensitive Yap/Taz transcriptional pathway in trabecular meshwork cells. *Investig Ophthalmol Vis Sci*. 2018;59(5):1969–1984.
34. Liton PB, Luna C, Bodman M, Hong A, Epstein DL, Gonzalez P. Induction of IL-6 expression by mechanical stress in the trabecular meshwork. *Biochem Biophys Res Commun*. 2005;337(4):1229–1236.
35. Igarashi N, Honjo M, Yamagishi R, et al. Involvement of autotaxin in the pathophysiology of elevated intraocular pressure in Posner-Schlossman syndrome. *Sci Rep*. 2020;10(1):6265.
36. Honjo M, Igarashi N, Kurano M, et al. Autotaxin–lysophosphatidic acid pathway in intraocular pressure regulation and glaucoma subtypes. *Investig Ophthalmol Vis Sci*. 2018;59(2):693–701.
37. Aikawa S, Hashimoto T, Kano K, Aoki J. Lysophosphatidic acid as a lipid mediator with multiple biological actions. *J Biochem*. 2015;157(2):81–89.
38. Sheng X, Yung YC, Chen A, Chun J. Lysophosphatidic acid signalling in development. *Dev*. 2015;142(8):1390–1395.
39. van Meeteren LA, Moolenaar WH. Regulation and biological activities of the autotaxin-LPA axis. *Prog Lipid Res*. 2007;46(2):145–160.
40. Ho LTY, Osterwald A, Ruf I, et al. Role of the autotaxin-lysophosphatidic acid axis in glaucoma, aqueous humor drainage and fibrogenic activity. *Biochim Biophys Acta Mol Basis Dis*. 2020;1866(1):165560.
41. Dupont S, Morsut L, Aragona M, et al. Role of YAP/TAZ in mechanotransduction. *Nature*. 2011;474(7350):179–184.
42. Raghunathan VK, Morgan JT, Dreier B, et al. Role of substratum stiffness in modulating genes associated with extracellular matrix and mechanotransducers YAP and TAZ. *Investig Ophthalmol Vis Sci*. 2013;54(1):378–386.
43. Pocaterra A, Romani P, Dupont S. YAP/TAZ functions and their regulation at a glance. *J Cell Sci*. 2020;133(2):jcs230425.
44. Yemanyi F, Vranka J, Raghunathan VK. Crosslinked extracellular matrix stiffens human trabecular meshwork cells via dysregulating β-catenin and YAP/TAZ signaling pathways. *Investig Ophthalmol Vis Sci*. 2020;61(10):41.
45. Valle ML, Dworshak J, Sharma A, Ibrahim AS, Al-Shabrawey M, Sharma S. Inhibition of interleukin-6 trans-signaling prevents inflammation and endothelial barrier disruption in retinal endothelial cells. *Exp Eye Res*. 2019;178:27–36.
46. Brooks GD, McLeod L, Alhayyani S, et al. IL6 trans-signaling promotes KRAS-driven lung carcinogenesis. *Cancer Res*. 2016;76(4):866–876.
47. Chen W, Yuan H, Cao W, et al. Blocking interleukin-6 trans-signaling protects against renal fibrosis by suppressing STAT3 activation. *Theranostics*. 2019;9(14):3980–3991.

Investigative Ophthalmology & Visual Science

48. Ohira S, Inoue T, Shobayashi K, Iwao K, Fukushima M, Tanihara H. Simultaneous increase in multiple proinflammatory cytokines in the aqueous humor in neovascular glaucoma with and without intravitreal bevacizumab injection. *Investig Ophthalmol Vis Sci*. 2015;56(6):3541–3548.
49. Takai Y, Tanito M, Ohira A. Multiplex cytokine analysis of aqueous humor in eyes with primary open-angle glaucoma, exfoliation glaucoma, and cataract. *Investig Ophthalmol Vis Sci*. 2012;53(1):241–247.
50. Garbers C, Rose-John S. Dissecting interleukin-6 classic- and trans-signaling in inflammation and cancer. *Methods Mol Biol*. 2018;1725:127–140.
51. Garbers C, Aparicio-Siegmund S, Rose-John S. The IL-6/gp130/STAT3 signaling axis: recent advances towards specific inhibition. *Curr Opin Immunol*. 2015;34:75–82.
52. Alvarado J, Murphy C, Juster R. Trabecular meshwork cellularity in primary open-angle glaucoma and nonglaucomatous normals. *Ophthalmology*. 1984;91(6):564–579.
53. Sivashanmugam P, Tang L, Daaka Y. Interleukin 6 mediates the lysophosphatidic acid-regulated cross-talk between stromal and epithelial prostate cancer cells. *J Biol Chem*. 2004;279(20):21154–21159.
54. Zhao Y, He D, Saatian B, et al. Regulation of lysophosphatidic acid-induced epidermal growth factor receptor transactivation and interleukin-8 secretion in human bronchial epithelial cells by protein kinase Cδ, lyn kinase, and matrix metalloproteinases. *J Biol Chem*. 2006;281(28):19501–19511.
55. Keller KE, Bhattacharya SK, Borrás T, et al. Consensus recommendations for trabecular meshwork cell isolation, characterization and culture. *Exp Eye Res*. 2018;171:164–173.
56. Stamer WD, Clark AF. The many faces of the trabecular meshwork cell. *Exp Eye Res*. 2017;158:112–123.
57. Futakuchi A, Inoue T, Wei FY, et al. YAP/TAZ are essential for TGF-β2–mediated conjunctival fibrosis. *Investig Ophthalmol Vis Sci*. 2018;59(7):3069–3078.
58. Chen WS, Cao Z, Krishnan C, Panjwani N. Verteporfin without light stimulation inhibits YAP activation in trabecular meshwork cells: implications for glaucoma treatment. *Biochem Biophys Res Commun*. 2015;466(2):221–225.
59. Al-Moujahed A, Brodowska K, Stryjewski TP, et al. Verteporfin inhibits growth of human glioma in vitro without light activation. *Sci Rep*. 2017;7(1):7602.
60. He FF, Bao D, Su H, et al. IL-6 increases podocyte motility via MLC-mediated focal adhesion impairment and cytoskeleton disassembly. *J Cell Physiol*. 2018;233(9):7173–7181.
61. Debidda M, Wang L, Zang H, Poli V, Zheng Y. A role of STAT3 in Rho GTPase-regulated cell migration and proliferation. *J Biol Chem*. 2005;280(17):17275–17285.
62. Pattabiraman PP, Rao PV. Mechanistic basis of Rho GTPase-induced extracellular matrix synthesis in trabecular meshwork cells. *Am J Physiol Cell Physiol*. 2009;298(3):749–763.
63. Rao PV, Pattabiraman PP, Kopczynski C. Role of the Rho GTPase/Rho kinase signaling pathway in pathogenesis and treatment of glaucoma: bench to bedside research. *Exp Eye Res*. 2017;158:23–32.
64. Vranka JA, Staverosky JA, Reddy AP, et al. Biomechanical rigidity and quantitative proteomics analysis of segmental regions of the trabecular meshwork at physiologic and elevated pressures. *Investig Ophthalmol Vis Sci*. 2018;59(1):246–259.
65. Raghunathan VK, Eaton JS, Christian BJ, et al. Biomechanical, ultrastructural, and electrophysiological characterization of the non-human primate experimental glaucoma model. *Sci Rep*. 2017;7(1):14329.
66. Yang YF, Sun YY, Acott TS, Keller KE. Effects of induction and inhibition of matrix cross-linking on remodeling of the aqueous outflow resistance by ocular trabecular meshwork cells. *Sci Rep*. 2016;6:30505.
67. Bonnans C, Chou J, Werb Z. Remodelling the extracellular matrix in development and disease. *Nat Rev Mol Cell Biol*. 2014;15(12):786–801.
68. Buczek-Thomas JA, Rich CB, Nugent MA. Hypoxia induced heparan sulfate primes the extracellular matrix for endothelial cell recruitment by facilitating vegf-fibronectin interactions. *Int J Mol Sci*. 2019;20(20):5065.
69. Kasetti RB, Maddineni P, Patel PD, Searby C, Sheffield VC, Zode GS. Transforming growth factor β2 (TGFβ2) signaling plays a key role in glucocorticoid-induced ocular hypertension. *J Biol Chem*. 2018;293(25):9854–9868.
70. Hernandez H, Medina-Ortiz WE, Luan T, Clark AF, McDowell CM. Crosstalk between transforming growth factor beta-2 and toll-like receptor 4 in the trabecular meshwork. *Investig Ophthalmol Vis Sci*. 2017;58(3):1811–1823.
71. Castelino FV, Bain G, Pace VA, et al. An autotaxin/lysophosphatidic acid/interleukin-6 amplification loop drives scleroderma fibrosis. *Arthritis Rheumatol*. 2016;68(12):2964–2974.
72. Hao F, Tan M, Wu DD, Xu X, Cui MZ. LPA induces IL-6 secretion from aortic smooth muscle cells via an LPA 1-regulated, PKC-dependent, and p38α-mediated pathway. *Am J Physiol Hear Circ Physiol*. 2010;298(3):H974–83.
73. Pattabiraman PP, Inoue T, Rao PV. Elevated intraocular pressure induces Rho GTPase mediated contractile signaling in the trabecular meshwork. *Exp Eye Res*. 2015;136:29–33.
74. Babizhayev MA, Brodskaya MW. Fibronectin detection in drainage outflow system of human eyes in ageing and progression of open-angle glaucoma. *Mech Ageing Dev*. 1989;47(2):145–157.
75. Faralli JA, Filla MS, Peters DM. Role of fibronectin in primary open angle glaucoma. *Cells*. 2019;8(12):1518.
76. Kasetti RB, Maddineni P, Millar JC, Clark AF, Zode GS. Increased synthesis and deposition of extracellular matrix proteins leads to endoplasmic reticulum stress in the trabecular meshwork. *Sci Rep*. 2017;7(1):14951.
77. Tektas OY, Lütjen-Drecoll E. Structural changes of the trabecular meshwork in different kinds of glaucoma. *Exp Eye Res*. 2009;88(4):769–775.
78. Dickerson J, Steely H, English-Wright S, Clark A. The effect of dexamethasone on integrin and laminin expression in Cultured human trabecular meshwork cells. *Exp Eye Res*. 1998;66:731–738.
79. Steely HT, Browder SL, Julian MB, Miggans ST, Wilson KL, Clark AF. The effects of dexamethasone on fibronectin expression in cultured human trabecular meshwork cells. *Investig Ophthalmol Vis Sci*. 1992;33(7):2242–2250.
80. Faralli JA, Filla MS, McDowell CM, Peters DM. Disruption of fibronectin fibrillogenesis affects intraocular pressure (IOP) in BALB/cJ mice. *PLoS One*. 2020;15(8):e0237932.
81. Hernandez MR, Ye H, Roy S. Collagen type IV gene expression in human optic nerve heads with primary open angle glaucoma. *Exp Eye Res*. 1994;59(1):41–52.
82. Konstas AGP, Marshall GE, Lee WR. Iris vasculopathy in exfoliation syndrome: an immunocytochemical study. *Acta Ophthalmol*. 1991;69(4):472–483.
83. De Groef L, Andries L, Siwakoti A, et al. Aberrant collagen composition of the trabecular meshwork results in reduced aqueous humor drainage and elevated IOP in MMP-9 null mice. *Investig Ophthalmol Vis Sci*. 2016;57(14):5984–5995.
84. Ho SL, Dogar GF, Wang J, et al. Elevated aqueous humour tissue inhibitor of matrix metalloproteinase-1 and connective tissue growth factor in pseudoexfoliation syndrome. *Br J Ophthalmol*. 2005;89(2):169–173.

Investigative Ophthalmology & Visual Science

85. Tang C, Takahashi-Kanemitsu A, Kikuchi I, Ben C, Hatakeyama M. Transcriptional co-activator functions of YAP and TAZ are inversely regulated by tyrosine phosphorylation status of parafibromin. *iScience*. 2018;1:1–15.
86. Hong JH, Hwang ES, McManus MT, et al. TAZ, a transcriptional modulator of mesenchymal stem cell differentiation. *Science*. 2005;309(5737):1074–1078.
87. Hayashi H, Higashi T, Yokoyama N, et al. An imbalance in TAZ and YAP expression in hepatocellular carcinoma confers cancer stem cell-like behaviors contributing to disease progression. *Cancer Res*. 2015;75(22):4985–4997.
88. Zegeye MM, Lindkvist M, Fälker K, et al. Activation of the JAK/STAT3 and PI3K/AKT pathways are crucial for IL-6 trans-signaling-mediated pro-inflammatory response in human vascular endothelial cells. *Cell Commun Signal*. 2018;16(1):55.

Investigative Ophthalmology & Visual Science